PHILOSOPHICAL TRANSACTIONS OF THE ROYAL SOCIETY B BIOLOGICAL SCIENCES

Chemico–structural phylogeny of the discinoid brachiopod shell

A. Williams, M. Cusack and J. O. Buckman

Phil. Trans. R. Soc. Lond. B 1998 **353**, 2005-2038
doi: 10.1098/rstb.1998.0350

THE ROYAL SOCIETY

Chemico-structural phylogeny of the discinoid brachiopod shell

Alwyn Williams, Maggie Cusack and James O. Buckman

Department of Geology and Applied Geology, University of Glasgow, Glasgow G12 8QQ, UK

CONTENTS **PAGE**

1. Introduction 2006
2. Terminology of shell structure 2007
3. Results 2007
   (a) Shell structure of *Discinisca* 2007
   (b) Shell structure of other living discinids 2017
   (c) Shell structure of post-Palaeozoic fossil discinids 2018
   (d) Shell structure of Palaeozoic discinoids 2019
   (e) Shell structure of trematids 2025
   (f) Chemistry of the discinoid shell 2025
4. Conclusions 2029
   (a) Transformations of periostracum and primary layer 2029
   (b) Transformations of the secondary layer 2030
   (c) Phylogeny of the discinoid shell 2030
Appendix A. Materials 2032
Appendix B. Methods 2034
   (a) Water and organic content of shells 2034
   (b) Mineral identification 2034
   (c) Microbial contamination 2034
   (d) Extraction of mineral-associated proteins of *D. tenuis* 2035
   (e) Tablets of larval valves of *D. tenuis* 2036
Appendix C. Data used in phylogenetic analysis 2036
   (a) The states of 38 characters used in the phylogenetic analysis of nine discinoid and three other lingulide genera listed in Appendix C(b) 2036
   (b) Matrix of 38 characters listed in Appendix C(a), among nine discinoid and three other lingulide genera 2037
References 2037

Stratiform shells of living discinids are composed of membranous laminae and variously aggregated, protein-coated granules of apatitic francolite supported by proteinaceous and chitinous nets in glycosaminoglycans (GAGs) to form laminae in rhythmic sets. The succession is like that of living lingulids but differs significantly in the structure of the periostracum, the nature of baculate sets and in its organic composition. In particular, discinids have a higher level of amino acids although with relatively lower acidic and higher basic concentrations; and their overall lower organic content is owing to lower levels of hydrophilic components, like GAGs and chitin. The organic constituents are not completely degraded during fossilization; but data are presently too meagre to distinguish between linguloid and discinoid ancestries.

Many differences among three of the four described extant genera emanate from transformations with a long geological history. *Pelagodiscus* is characterized by regular, concentric rheomorphic folding (fila) of the flexible periostracum and the plastic primary layer and by sporadically developed hemispherical imprints of periostracal vesicles. Both features are more strikingly developed in Palaeozoic discinids. In the oldest discinid, the Ordovician *Schizotreta*, and the younger *Orbiculoidea* and related genera, vesicles were persistent, hexagonal close-packed arrays fading out over fila. They must have differed in composition, however, as the larger vesicles of *Schizotreta* were simple (possibly mucinous), whereas the smaller vesicles of *Orbiculoidea* and younger genera were composites of thickly coated spheroids, possibly of lipoproteins, which survive as disaggregated relicts in *Pelagodiscus*. Baculate sets within the secondary layer are also less well developed in living discinids, being incipient in *Pelagodiscus* and restricted to the dorsal valve of *Discinisca*. The trellised rods (baculi) with proteinaceous cores are

Received 13 June 1997 *Accepted* 9 September 1997

composed of pinacoids or prisms of apatite, depending on whether they are supported by chitinous nets or proteinaceous strands in GAGs. This differentiation occurred in *Schizotreta* but in that stock (and *Trematis*) the baculate set is symmetrical with baculi subtended between compact laminae, whereas in younger and post-Palaeozoic species the outer bounding lamina(e) of the set is normally membranous and/or stratified. The most striking synapomorphy of living discinids is the intravesicular secretion of organosiliceous tablets with a crystalline habit within the larval outer epithelium and their exocytosis as a close- or open-packed, transient, biomineral cover for larvae. Canals, on the other hand, are homologous with those pervading lingulid shells. Both systems interconnect with chitinous and proteinaceous sets and have probably always served as vertical struts in an organic scaffolding supporting the stratiform successions.

A phylogenetic analysis based mainly on shell structure confirms the discinoids as the sister group of the linguloids but, contrary to current taxonomic practice, also supports the inclusion of acrotretoids within a 'discinoid' clade as a sister group to the discinids.

Keywords: organophosphatic; siliceous brachiopods; chemico-structural shell phylogeny

1. INTRODUCTION

Discinoids, linguloids and rhynchonellides are the only living brachiopods with intra-ordinal early Palaeozoic ancestors. The inarticulated, organophosphatic-shelled discinoids and linguloids differ fundamentally from the articulated, organocalcitic rhynchonellides. Discinoid and linguloid shells are also morphologically distinguishable from each other in the growth of their ventral valves and the way they accommodate the pedicle. Consequently, discinoids and linguloids have been traditionally regarded as only distantly related through some extinct acrotretoid (Williams & Rowell 1965).

Recently a much closer relationship has been favoured by L. E. Holmer and L. E. Popov (personal communication) who postulate that the discinoids were 'derived directly from within the Lingulida'. Among the features cited in support of a lingulide ancestry for discinoids is the chemico-structure of the shell. Some aspects of the integuments of the two stocks, however, are not compatible with a total homology. The periostracum of living discinids and lingulids are different (Williams & MacKay 1979) and the shells of both groups, although stratiform in fabric, are characterized by distinctive laminae (Williams *et al*. 1992, 1994). Comparative biochemical studies of the shells of fossil and living discinoids and linguloids (Jope 1965, 1980) also reveal differences in the proportions of amino acids between the two groups.

During the last decade or so, the lingulid integument has been widely studied (Iwata 1981; Pan & Watabe 1988; Williams *et al*. 1994; Cusack & Williams 1996) and can be used to recognize a 'sister group' to reconstruct the chemico-structural phylogeny of the discinoid shell. Such a comparative investigation is opportune, as much work has recently been done on the evolution and systematics of early Palaeozoic inarticulated brachiopods including investigations of the shell microfabrics of acrotretoids (Holmer 1989; Popov 1992; Popov & Ushatiniskaya 1992; Williams & Holmer 1992; Holmer & Popov 1996), which have also been favoured as the discinoid stem group.

Despite the great geological range of discinoids, from Early Ordovician to Recent, their genealogy involves comparatively few genera assigned to two families, the Trematidae and Discinidae (figure 28). A total of seven genera have been recorded coevally in Lower and Middle Palaeozoic successions compared with four at the present time. There is also a significant break in the discinoid geological record. Only one of the Recent genera, '*Discinisca*', has been identified in Mesozoic successions but not yet in sediments of Triassic age; while only two Palaeozoic discinoids, *Oehlertella* and *Orbiculoidea*, are known from rocks as young as the Permian. In respect of shell morphology, this break in the record of discinoid genealogy is not important as any of the late Palaeozoic stocks could have been ancestral to Recent species. In terms of shell structure, however, there is a basic distinction between the presence of superficial, microscopic pits on the post-larval shells of some Palaeozoic discinoids (Holmer 1987; Williams & Curry 1991) and their absence in post-Palaeozoic genera other than *Pelagodiscus*. These pits have been interpreted as casts of periostracal vesicles. They are well developed on the larval shells of acrotretoids (Biernat & Williams 1970; Holmer 1989) and on the post-larval shells of some linguloids (Holmer 1986). The pits, therefore, afford a means of sorting out some aspects of organophosphatic shell differentiation.

Variations in shell fabric were another source of ultrastructural checks of the phylogenetic relationship between discinoids and linguloids. In particular, baculate laminae are found in some living and fossil linguloids as well as in discinoids; but whether they are homologous and secreted in the same way as the columnar laminae of acrotretoids has not been explored. Preliminary investigations by us have shown that the superficial fine structure of the baculi of the linguloid *Glottidia* is not the same as that of living discinids. There was, therefore, the prospect of determining the phylogenetic origin of all such differences and comparing the genealogy so derived with those supported by investigations of periostracal ultrastructures and shell biochemistry.

The structure and emphasis of this paper have been determined by the availability of adequate samples of discinoids as well as by the aim of the investigation. *Discinisca* has been used as the prime source of information on the living integument of the superfamily, despite the fact that the terminology of discinoid shell structure was first established for *Discina* (Williams *et al*. 1992). Several extant species of *Discinisca* are known from mid- to low latitudinal, inter-tidal and off-shore regions of the circum-Pacific, the Caribbean and the south Atlantic and Indian Oceans. In contrast, the monotypic *Discina* is restricted to West African tropical waters, while

other living discinids are even rarer. The shell structure of Palaeozoic discinids is comprehensively represented by *Orbiculoidea* which is cosmopolitan in distribution and probably ranged from the Ordovician to Permian inclusive. The trematids, on the other hand, are comparatively rare and insufficient samples could be obtained to undertake a full chemico-structural investigation of the family.

The aim of this study, to establish a chemico-structural genealogy for discinoid shells, has also determined the scope of our investigations of the living integument. We have concentrated on those chemico-structural features of the shell, which are likely to have survived fossilization. We have, therefore, been more concerned with determining and correlating discinoid shell successions than with those other aspects of the integument, such as the attachment of muscle systems, which are not an integral part of biomineralization.

2. TERMINOLOGY OF SHELL STRUCTURE

In 1992 (Williams *et al*. 1992, pp. 85–87), an attempt was made to standardize the terminology used to describe the microtexture and successions of shells of organophosphatic brachiopods. There were two reasons for doing so. First, there are many units of successions characterized by distinctive microtextures which reflect differences in the cytology and biochemistry of the secreting epithelium and which were already known to have had a long geological history. Second, terminological recognition of the more persistent microtextures is an essential aid in the phylogenetic analysis of the chemico-structural evolution of the shell.

So far as is known, the organophosphatic shell has always been composed of a succession of distinctive units (laminae), normally of very great areas compared with their thicknesses and disposed at low angles to valve curvature (stratiform succession). Laminae are, therefore, isomorphous sheets and have been named after the most distinctive configuration of their biomineral or organic constituents—compact, botryoidal, rubbly, rod and plate (virgose), baculate, stratified, membranous and so on (Williams *et al*. 1992, 1994; Cusack & Williams 1996).

There is, however, a disadvantage to considering each lamina in isolation. Stratiform successions are normally composed of rhythmic sequences of laminae, repeated in full or in various combinations, which are the outcome of a cyclical secretion by mantle epithelium. The composition of these rhythmic groups can change laterally and/or vertically within a shell as well as from one genealogy to another; but their identification is essential in attempting to trace the phylogeny of secretory regimes. We use the term 'set' to embrace all laminae making up such a group, which is named after the structurally dominant lamina within the sequence.

3. RESULTS

The following account of the living discinid integument is based on studies of the shell and mantle of *Discinisca tenuis* (Sowerby) and *D. lamellosa* (Broderip). Pervasive canal systems are also well seen in *Discina striata* (Schumacher) and their description is based on data from both genera. The shell structure of the rare, abyssal *Pelagodiscus atlanticus* (King) is then outlined before Cenozoic and Mesozoic discinid species are discussed.

Table 1. *Water and organic content of three species of discinoid brachiopods as compared with the linguloid brachiopods*, Lingula anatina *and* Glottidia pyramidata

	water	organic (% wet weight)	organic (% dry weight)
Discinisca tenuis	8.5	32.1	25.7
Discinisca lamellosa	6.8	31.5	26.5
Discina striata	6.1	41.1	37.3
Lingula anatina	9.7	42.2	35.9
Glottidia pyramidata	12.5	61.0	55.4

The shells of 12 species of Palaeozoic discinids have been investigated. Those of *Orbiculoidea* and *Schizotreta* have provided the most complete information on the chemico-structure of ancestral discinids. The stratiform successions of other Palaeozoic discinids do not vary significantly from those of the *Orbiculoidea* model.

Well-preserved samples of the extinct trematids were too small to provide as much chemico-structural data as were obtained from contemporaneous discinids. Details of shell structure, however, have helped to postulate the origin of the discinoid integument.

(a) *Shell structure of* Discinisca

The mature shell of living *Discinisca* comprises many organic and mineral components, some of which are visually distinctive. They aggregate into a stratiform succession of laminae, normally no more than a few microns thick but traceable over areas of several square millimetres. The chemico-structure of the *Discinisca* larval shell is sufficiently distinctive to merit a separate note.

(i) *Mineral constituents*

The organic content of the shell of *Discinisca tenuis*, at 32.1% by weight, is less than that of *Lingula anatina* at 42.2%. The organic content of *Discinisca lamellosa* and *Discina striata* are 31.5% and 41.1%, respectively (table 1). The overall composition of *D. lamellosa* and *L. anatina* is broadly the same (Jope 1965, p. H158). In *D. tenuis* the most easily identifiable structural components of the shell are apatite, glycosaminoglycans (GAGs), and proteinaceous strands.

The basic apatitic unit of the discinid shell is a granule (see figure 11*b*), 4–8 nm in diameter. The X-ray diffraction patterns of this biomineral in the shells of *D. tenuis*, *D. lamellosa*, *D. striata* (figure 1), are all comparable with those of *Glottidia pyramidata* and *L. anatina* obtained by LeGeros (1985, p. 99) who, using infrared (IR) absorption and fluorine analyses, described the mineral component of the two lingulids as 'crystallo-chemically similar but not identical to marine phosphorite or mineral francolite, a CO_3-containing calcium fluorapatite'.

Transmission electron microscope (TEM) sections of the shell of *D. tenuis* (figure 2*e*) show that the granules are associated with proteins and aggregate into spherules

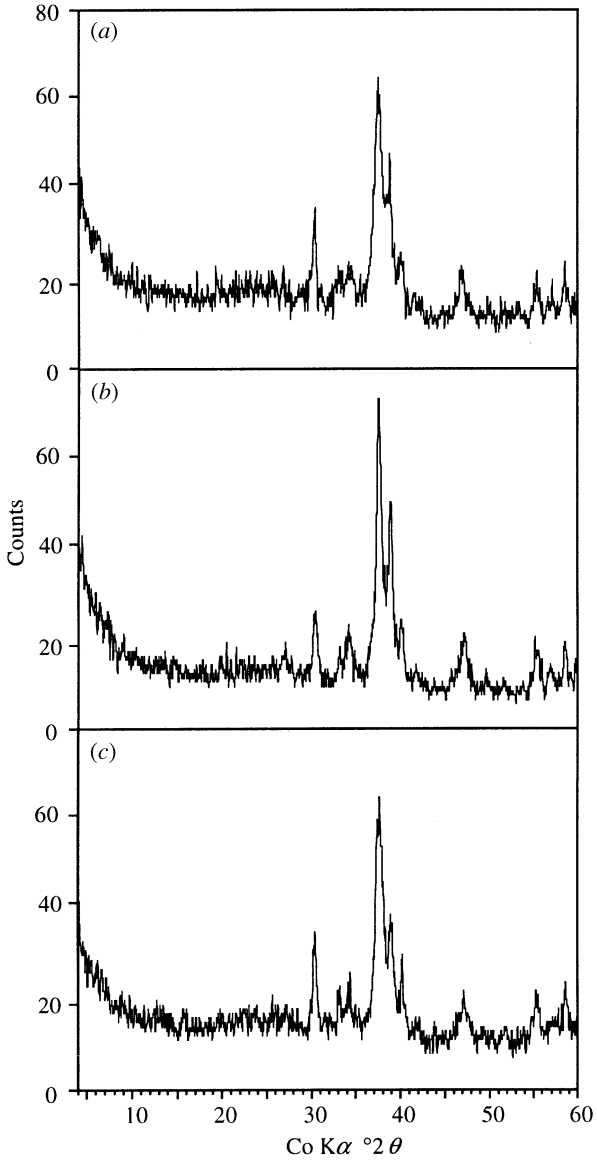

Figure 1. X-ray diffraction (XRD) line profiles of discinid shells (*a*) *Discinisca tenuis*, (*b*) *D. lamellosa*, and (*c*) *Discina striata*. Shells powdered in acetone were poured over glass slides and XRD determinations were made in a Philips PW 1050/35 XRD with a Co energy source.

(figure 2*a*), typically 40 nm in diameter, but exceptionally occurring as mosaics up to 500 nm in size. In compacted layers, these bodies normally fit together in hexagonal close-packed arrangements (or exceptionally interlocking like platy jigsaw pieces (figure 2*b*)) and, more rarely, as rods 100–500 nm long (figure 2*d*). Sections under the scanning electron microscope (SEM) as well as the TEM show that spherules and mosaics are organically coated as are the rod-like arrangements of spherules.

The dominant organic constituents of the *Discinisca* shell are GAGs. They fill all spaces within the biomineral framework of the shell and constitute much of the organic fraction identified by Iijima and co-workers (1991), in their analysis of the *Lingula* shell, as being rich in galactosamine. Structurally, GAGs are featureless except for dehydration cracks and, as infills, may vary from sheets up to several microns thick to ellipsoidal or sub-circular bodies about one micron in diameter. Such discrete bodies of GAGs are found in buffered as well as enzyme-digested sections (figure 2*a*). As noted in Appendix B, GAGs may contain spherules or be indented by spherular substrates when occurring as films. On internal surfaces, rounded masses of GAGs can be found surrounding canals (figure 2*a*) in a continuity suggestive of vesicular discharges exuded simultaneously with the secretion of the canal walls.

The third kind of structural constituents are various membranes (figures 2*c*, 3*a*), meshes (figure 7*f*) and strands (figure 3*b*). The membranes are digested by proteinase-K and the meshes exposed without apparent degradation by subtilisin; they have been respectively identified as proteinaceous and chitinous. The strands are 30–60 nm thick and are sporadically threaded through GAGs and clusters of apatitic spherules. They are identical to strands found in the *Lingula* shell, which have been compared with an actin-like protein (Cusack & Williams 1996).

(ii) *Stratiform successions*

The periostracum of *D. tenuis* (figure 3*c*,*d*) is the same as that of other species of *Discinisca* (Williams & MacKay 1979) and acts as a substrate for the secretion of a primary layer. If the outer boundary of the secondary layer is defined as the interface at which canals terminate (Williams *et al*. 1994, p. 242), the *Discinisca* primary layer is almost entirely organic in composition and about 100 nm thick (figure 3*c*). However, it grades into the secondary layer through a zone, 3–10 μm thick, with abundant apatitic spherules which may be dispersed (figure 3*c*) or disposed in jigsaw patterns or rods up to 750 μm long but seldom as mosaics (figure 3*e*). This zone is generally identified as the primary layer especially in fossilized shells as it acts as a casting medium for superficial features of the shell, which are preserved in nanometric detail. They include persistent radial ridges (capillae) (figure 4*c*) with a wavelength of about 1.5 μm, sporadically broken by impersistent belts of concentrically disposed rheomorphic folds (figure 4*b*). Such micro-structures affect the periostracum and presumably represent, respectively, the imprints of arched tips of vesicular cells and periodic bucklings of the periostracum during its secretion at the mantle edge.

The secondary layer of *Discinisca*, like that of *Discina* (Williams *et al*. 1992), is composed of the same kind of lamination as in *Lingula*, except for the development of baculate laminae which are absent from the shell of *Lingula* although present in that of the related *Glottidia*. In discinids, baculate lamination is also differentially developed, occurring in both valves of *Discina* but only in the ventral valve of *Discinisca*.

The dominant secondary sequence consists of alternations of compact and rubbly laminae in sets normally 3 and 12 μm thick (figure 4*a*,*d*). As X-ray diffraction (XRD) readings confirm, the physical distinction between them relates to the close-packed spherules of the compact lamina in contrast to their greater dispersion within the higher organic content of the rubbly lamina. This is well shown in sections bleached to remove GAGs from chambers and galleries within the rubbly laminae especially around apatitic encased canals (figure 4*d*).

In fracture sections, distinctive cleavages characterize the compact and rubbly laminae, respectively (figure 5*a*). The

PHILOSOPHICAL TRANSACTIONS OF THE ROYAL SOCIETY B BIOLOGICAL SCIENCES

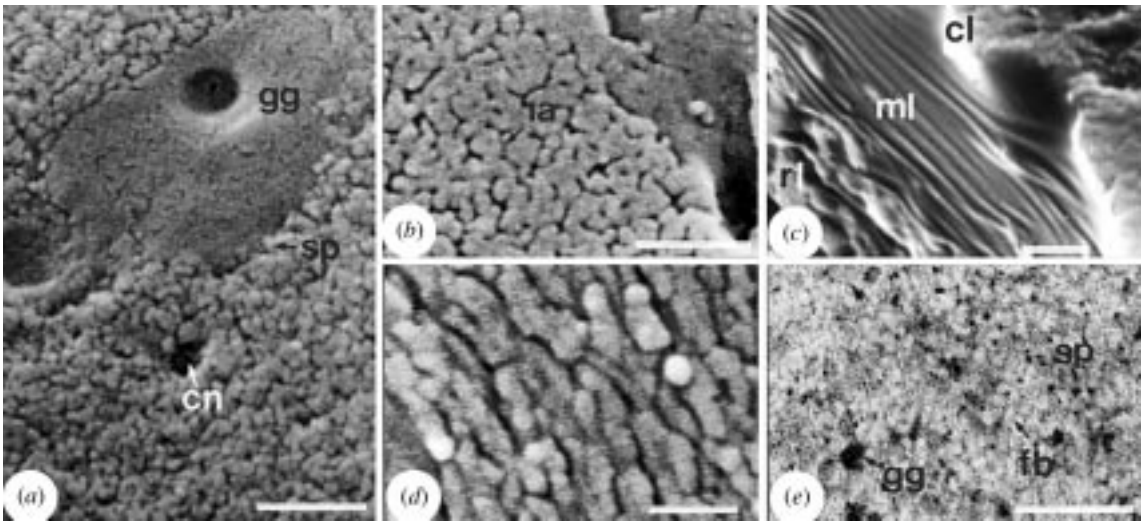

Figure 2. Scanning (*a–d*) and transmission (*e*) electron micrographs of structural components of the shell of *Discinisca tenuis*. (*a*, *b*) Gold-coated internal surfaces treated with buffer, showing spherular (sp) and interlocking (ia) apatite, canals (cn) and GAGs (gg); scale bars, 0.5 µm. (*c*) Bleached, resin-impregnated, vertical section showing membranous laminae (ml), between compact (cl) and rubbly (rl) laminae; scale bar, 1 µm. (*d*) Internal surface treated with proteinase-K showing rods of spherular apatite; scale bar, 250 nm. (*e*) Demineralized section of the primary layer showing electron-dense clots of GAGs (gg) with organically coated spherules (sp) and fibrils (fb); scale bar, 0.5 µm.

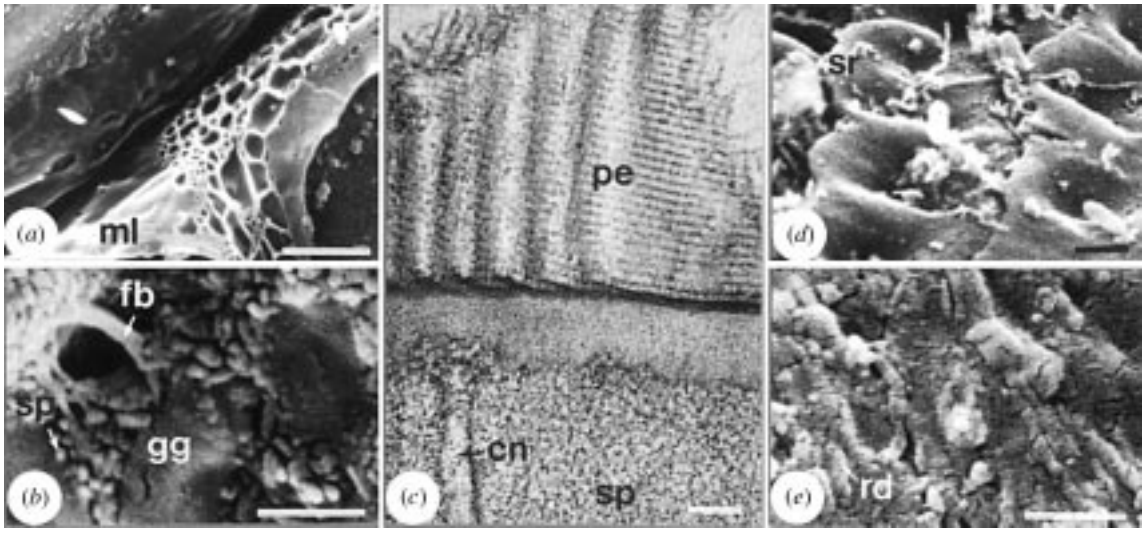

Figure 3. Scanning (*a*, *b*, *d*, *e*) and transmission (*c*) electron micrographs of the organic structural components and the periostracum and primary layer of *Discinisca tenuis*. (*a*) Vertical fracture section treated with bleach showing a membrane lamina (ml) with an internal 'bubble-raft' surface; scale bar, 5 µm. (*b*) Vertical fracture section treated with proteinase-K showing organic strands (fb), provisionally identified as 'actin', threaded through GAGs (gg) with aggregates of spherules (sp); scale bar, 0.5 µm. (*c*) Demineralized section of the periostracum (pe) composed of pellicular sheets, underlain by primary layer with organically coated spherules of apatite (sp) penetrated by a canal (cn) terminating at the interface between the periostracum and primary layer; scale bar, 100 nm. (*d*) Surface view of critical point dried scalloped ridges (sr) of periostracum; scale bar, 1 µm. (*e*) External view of primary layer treated with subtilisin with apatitic rods (rd) in GAGs; scale bar, 0.5 µm.

cleavage appears to be related to the distribution of GAGs which are impersistent and sheet-like in the former (figure 5*b*) and more pervasive and bulky in the latter laminae (figure 5*d*). As a result, the secondary layer of a mature shell commonly consists of two physically different zones (figure 5*a*). The outer succession with thicker compact laminae is more highly and obliquely cleaved with successive sets of cleavage planes opening in opposite directions. In the inner succession, where rubbly laminae become more important, a coarser, vertical cleavage predominates.

The passages between compact and adjacent rubbly laminae are commonly transitional (figure 5*c*). However, membranes, when they occur, cover the inner surface of a compact lamina (figure 5*c*) and may be indented like a negative bubble raft, possibly representing the imprints of compacted spherules and mosaics (figure 3*a*). Membranes may occur in sets (figure 2*c*) and may bear fibrous wisps, presumably also of chitin (figure 5*e*) when unaffected by subtilisin.

Laminae, composed of apatitic rods bound by variably biomineralized roofs and floors (baculate laminae), were first identified in Early Palaeozoic organophosphatic acrotretoids (Poulsen 1971), and confirmed by Holmer (1989). Similar structures have been described in *Glottidia*

PHILOSOPHICAL TRANSACTIONS OF THE ROYAL SOCIETY B BIOLOGICAL SCIENCES

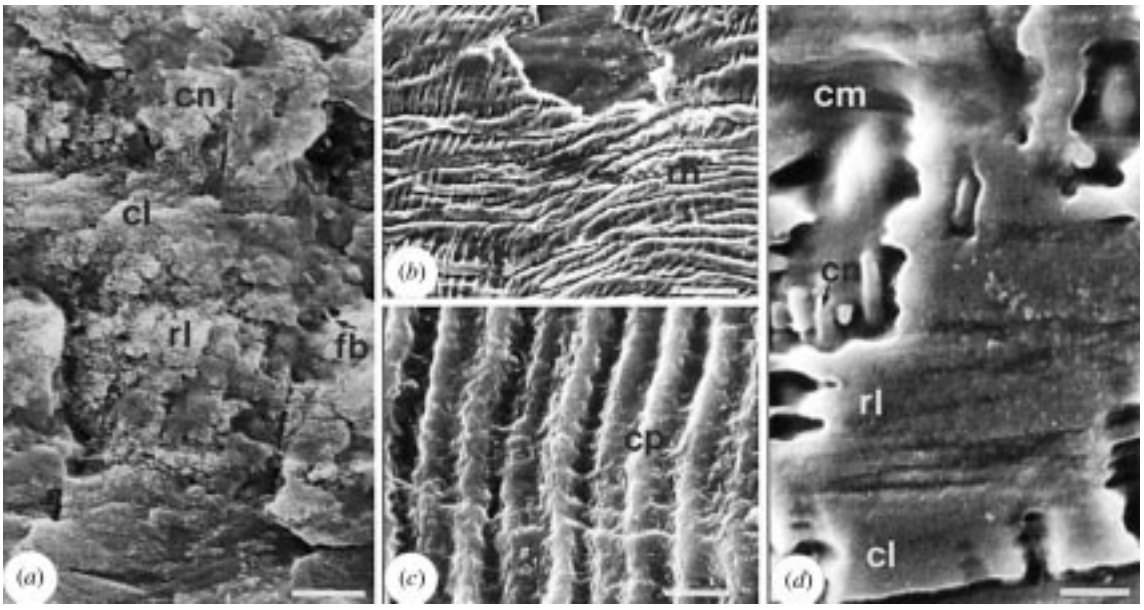

Figure 4. Scanning electron micrographs of the shells of *Discinisca tenuis* (*a*) and *D. lamellosa* (*b–d*). (*a*) Vertical fracture surface of secondary layer treated with proteinase-K, showing compact (cl) and rubbly (rl) laminae, strands of 'actin' (fb) and canals (cn); scale bar, 2 µm. (*b*, *c*) External views of dried valve showing rheomorphic folding (rh) and capillae (cp) of the periostracum and primary layer; scale bars, 50 µm and 5 µm, respectively. (*d*) Polished vertical section of resin-impregnated secondary layer treated with bleach, showing compact (cl) and rubbly (rl) laminae penetrated by canals (cn) and chambers (cm); scale bar, 5 µm.

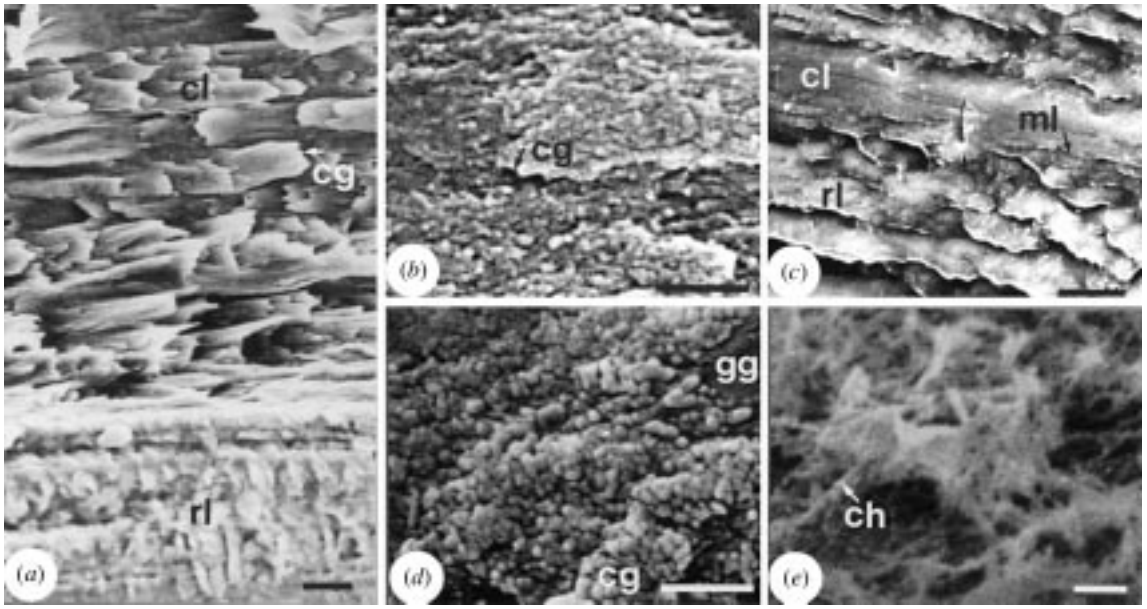

Figure 5. Scanning electron micrographs of the secondary layer of the shell of *Discinisca tenuis*. (*a*, *b*, *d*) Vertical fracture section treated with subtilisin and showing the effects of GAGs (gg) distribution on cleavage (cg) in compact laminae (cl), enlarged in (*b*), and rubbly laminae (rl), enlarged in (*d*); scale bars, 10 µm, 0.5 µm and 0.5 mm, respectively. (*c*) Polished vertical section of resin-impregnated secondary layer treated with bleach showing membranes (ml) interleaved with compact (cl) and rubbly (rl) laminae; scale bar, 5 µm. (*e*) External view of membranous laminae treated with subtilisin showing a disturbed layer of chitinous strands (ch); scale bar, 0.5 µm.

and *Discinisca laevis* (Sowerby) by Iwata (1982). TEM studies of the *Discina* shell (Williams *et al.* 1992, p. 99) revealed how baculi grow from a compact lamina as proteinaceous rods with closely distributed, coated granules of apatite and connected with one another by organic strands.

In *Discinisca*, baculate lamination is restricted to the outer layers of secondary shell within the body platform (and septum) of mature ventral valves. The baculi occur in rhythmic sets and are typically subtended between rubbly or compact laminae (figure 6*a*,*f*). The inner boundary of such a unit may be a succession of spherular-coated membranes (figures 6*d* and 7*c*) or a compact lamina with apatitic spherules aggregated into cylindroids, up to 200 nm long, at the interface (figure 7*a*). The outer boundary is commonly a less well defined

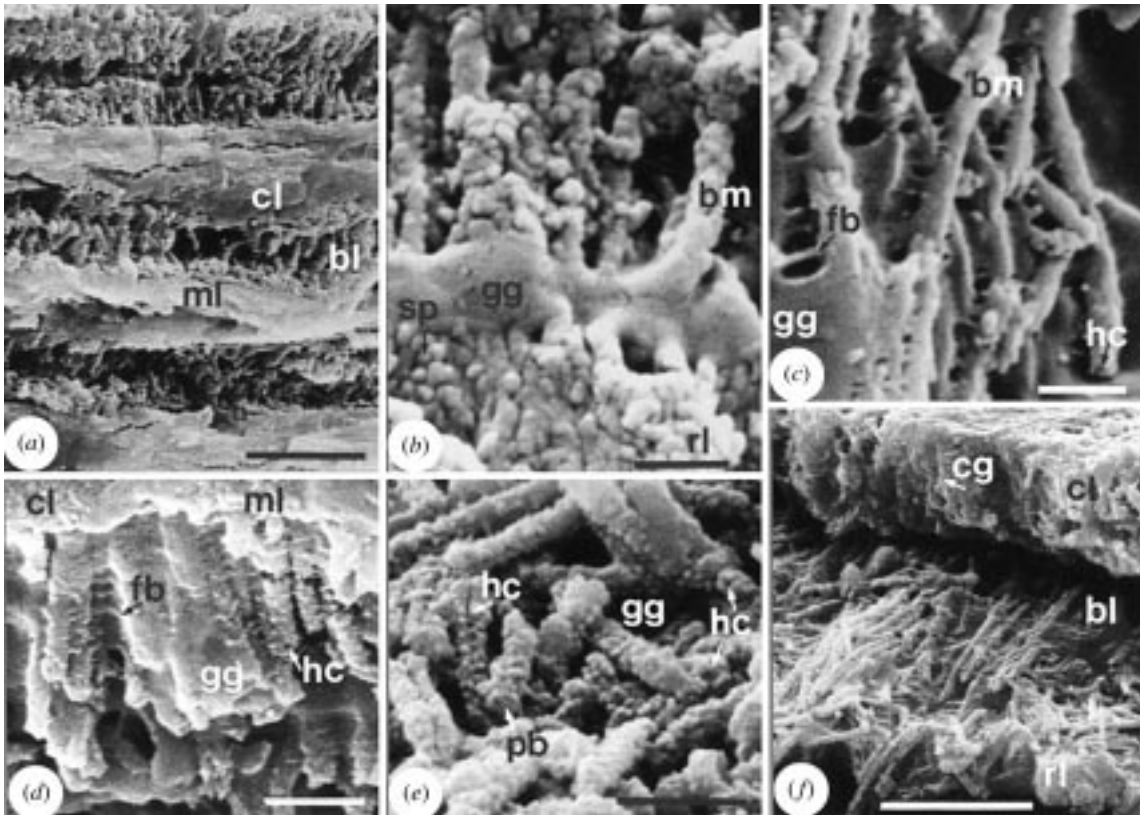

Figure 6. Scanning electron micrographs of baculate lamination in vertical fracture sections of the secondary layer of *Discinisca lamellosa* (*a–d*), and *D. tenuis* (*e*, *f*); all sections treated with subtilisin except that in (*f*) (buffered). (*a*) A succession of baculate laminae (bl) in relation to compact (cl) and membranous (ml) laminae; scale bar, 5 µm. (*b*, *c*) Baculi (bm), some with hollow cores (hc), embedded in GAGs (gg) and interconnected by 'actin' strands (fb), succeeded by a rubbly laminae (rl); scale bars, 0.5 µm. (*d*) Baculi with hollow cores (hc), embedded in GAGs (gg) and interconnected by 'actin' strands (fb), succeeding compact (cl) and membranous (ml) laminae; scale bar, 1 µm. (*e*) Broken baculi with some GAGs (gg) showing hollow cores (hc), and plugged baculi (pb); scale bar, 1 µm. (*f*) A collapsed baculate lamina (bl) succeeding a cleaved (cg) compact lamina (cl) and succeeded by a rubbly lamina (rl); scale bar, 5 µm.

transition with a high organic content. Such units represent a single cycle of deposition as in *Discina* (Williams *et al*. 1992, p. 100). The interpretation of such depositonal sequences depends on the secretion of membranes which are here recognized as the datum horizons marking a cycle of deposition. Individual baculi have a constant thickness commonly 150–250 nm (range 70–350 nm) and may exceed 5 µm in length (figure 6*b–d*). They are unbranched and are disposed vertically or at angles of 60° or so to the substrates to form a three-dimensional trelliswork which, in the living shell, is supported by the all-pervasive GAGs (figure 6*b*,*c*). In dead shells, the removal or shrinkage of GAGs by enzymic digestion or dehydration usually causes a partial collapse of the biomineralized framework and the fragmentation of baculi (figure 6*f*).

Baculate morphology is variable. The granular surfaces of most baculi, especially those held in place by radiating strands 20 nm or so thick, are studded with mosaics and cylindroids of spherular apatite (figure 7*b*,*e*). Some baculi, however, mainly consist of stacked pinacoids that grew in relation to very fine horizontal meshes (figure 7*c*,*f*). Both strands and meshes are exposed in an unimpaired state when the GAGs matrix of baculate laminae is digested in proteinase-K or subtilisin. In contrast, transverse sections of broken baculi digested by these proteases have hollow cores (about one-third the diameter of the rod) (figure 6*c–e*) or cores plugged by subcentral spherules (figure 6*e*). Transverse sections of broken baculi treated with buffered solutions, however, do not have hollow cores, only depressions within a cluster of spherules. In both enzymically digested and buffered laminae, some baculi are closed by narrow, rounded tips comprising spherules, and are interpreted as having been terminated during laminar secretion.

The differential digestion of the organic constituents of baculate laminae suggests that baculi have axial proteinaceous threads and that the protease-resistant strands and meshes are chitinous. Similar strands and meshes also support mosaics and short rods of spherular apatite in virgose laminae (compare figure 7*d*) and are likewise assumed to be chitinous.

(iii) Discinisca *larval shells*

The outer surfaces of the larval valves of *D. tenuis* undulate in low ripples, concentric to a posteriorly eccentric swelling about 40 µm in diameter ('bulla' of Holmer (1989)) and culminating in a raised margin, the 'halo' of Chuang (1977) (figure 8*a*). They are covered with concave or convex tablets and pits (figure 8*d*), approximating to an open hexagonal packing and extending to the halo where they fade.

The tablets are normally well displayed on dried larval shells. They are roundedly rhomboidal to elliptical in

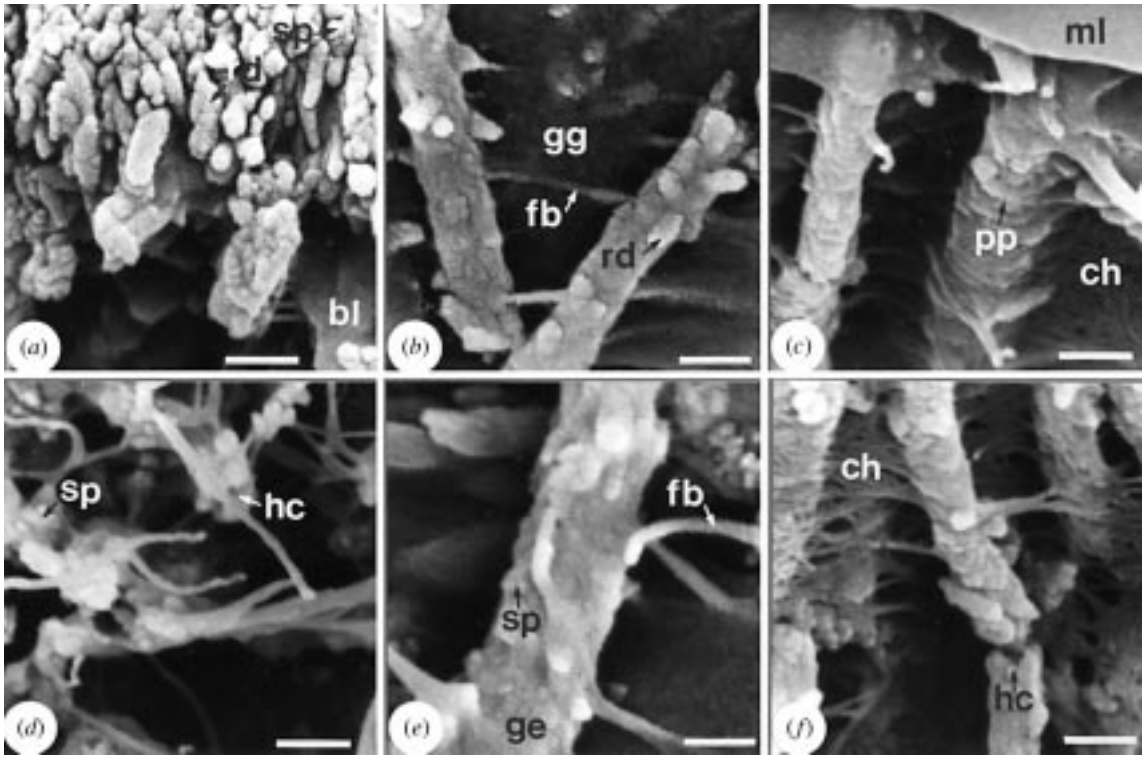

Figure 7. Scanning electron micrographs of baculi in vertical fracture sections of a ventral valve of *Discinisca tenuis* treated with subtilisin. (*a*) A compact lamina of granules, spherules (sp) and rods (rd) inwardly succeeded by a baculate lamina (bl); scale bar, 200 nm. (*b–f*) Baculi in GAGs (gg), composed of pinacoidal plates (pp) associated with nets of anastomosing fibrils identified as chitin (ch), or of granular (ge) spherules (sp) and rods simulating prisms (rd) associated with 'actin' strands (fb), and some broken baculi with hollow cores (hc); scale bars, 150 nm for all five micrographs except (*e*), 100 nm.

outline, with major and minor axes averaging 1.3 μm and 0.85 μm, respectively (figure 8*b*,*c*), and are up to 650 nm apart (figure 8*d*). They may be covered by a tension-cracked membrane bearing the imprints of spherules, 20–60 nm or so in diameter, on the outer surface of underlying tablets (figure 8*c*). Rupture of the membrane exposes rhomboidal, hexagonal or even ditetragonal tablets (figure 8*b*,*f*) about 70 nm thick. The tablets are usually concave externally and in various stages of drifting free of their original sites (figure 8*g*,*j*). They do, however, leave behind imprints on the floor of the larval primary layer which is composed of closely dispersed spherules in a cracked and pitted organic matrix (figure 8*b*,*c*). The imprints are usually gently convex centrally with incised margins; some margins are incompletely impressed suggesting they were made by tilted tablets (figure 8*g*). Similar imprints have been found on the larval shells of *Discina* (figure 9*a*) and *Pelagodiscus* (figure 9*b*,*c*). Those of *Pelagodiscus* are closely packed rhombohedral moulds, with sunken or raised inner surfaces, separated from one another by strips of apatitic substrate forming walls and grooves respectively, about 100 nm wide.

The tablets have all the characteristics (Lowenstam & Weiner 1989, p. 41) of having been secreted as completed structures within intracellular vesicles, in the manner of coccolith segments (Westbroek *et al*. 1984, p. 436). Their shape, however, is crystalline and so suggestive of pinacoids of calcite and aragonite as well as apatite that attempts have been made to determine their composition. The only available supply of abundant, well-preserved larval shells were those on immature specimens attached to dead, adult *D. tenuis* washed up in clusters on the beach at Swakopmund. They were used for several lines of investigation.

XRD of solid residues, recovered by immersing samples in distilled water, 0.5% bleach and subtilisin, found significant traces only of sodium chloride from sea water (and bleach). Energy dispersive X-ray (EDX) line counts did not distinguish exposed tablets from their surrounds in Na, Cl, or Mg. The peaks in spot counts on larval tablets and adult shell were virtually the same and reveal the presence of only apatite and some 'diatomaceous' silicon traces on the surfaces.

To ascertain the organic constituents of the tablets, three samples were treated with graded concentrations of subtilisin (up to 10 μM), chitinase (up to 10 μM) and bleach (up to 0.5% by volume) while a fourth was immersed in distilled water. The membrane covering the tablets degraded in 2 μM subtilisin, 1 μM chitinase and 0.2% bleach, and these concentrations also exposed apatitic spherules in the substrate. The membrane is, therefore, likely to be comparable with the fibrous components of the periostracum of the post-larval shell and the underlying primary layer. Exposed tablets were not digested by chitinase but were degraded by 2 μM subtilisin and by 0.2% bleach around their edges and on their surfaces (figure 8*h–j*) to reveal that the biomineral component consists of discrete granules or spherules in a proteinaceous matrix. Degradation of the organic constituents also reveals that a tablet is essentially a flat box (figure 8*h*) containing spherules which spill out from split tablets (figure 8*e*).

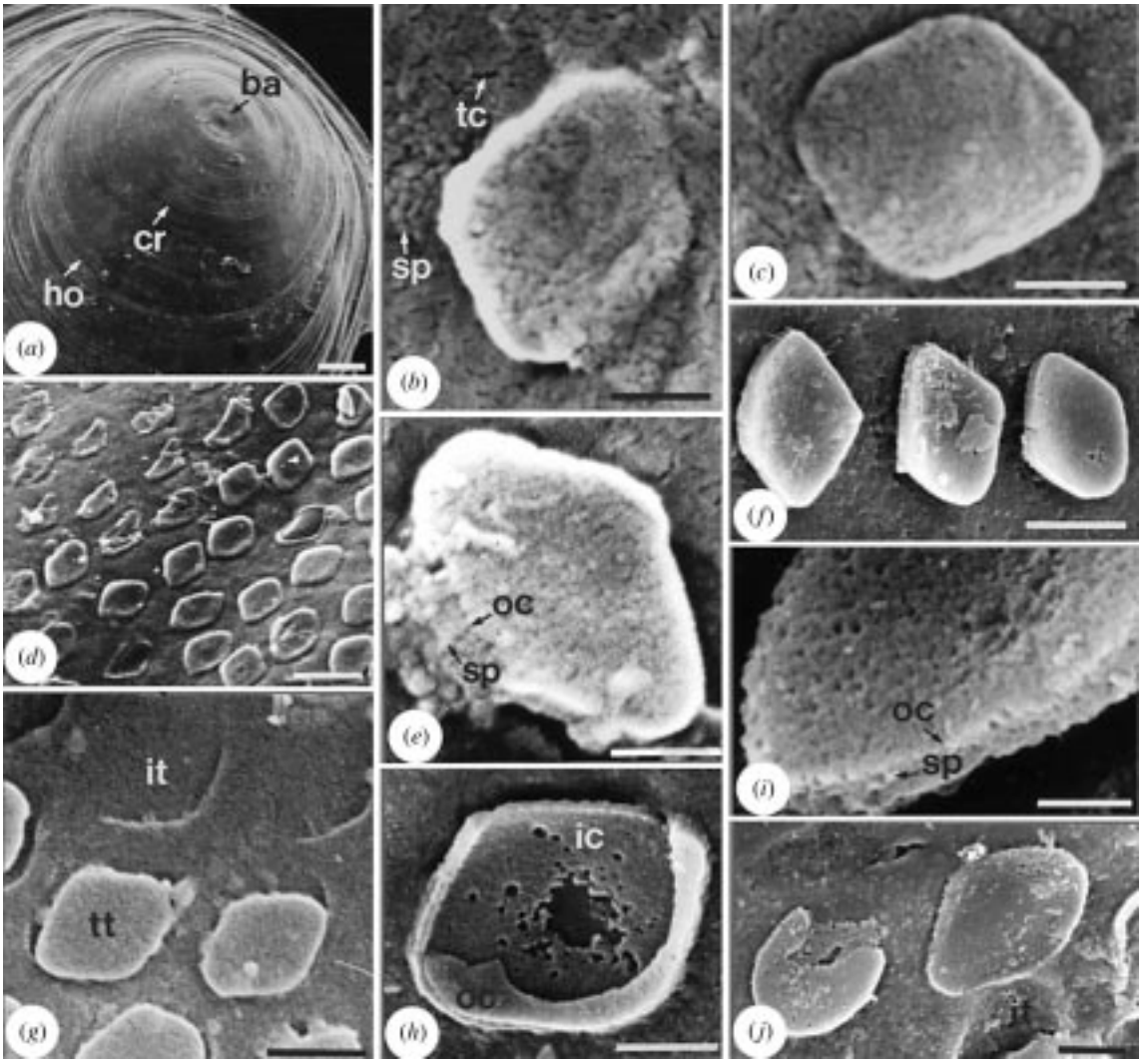

Figure 8. Scanning electron micrographs of larval shells of *Discinisca tenuis*. (*a*) Dried dorsal valve with halo (ho), concentric ripples (cr) and bulla (ba); scale bar, 100 µm. (*b*, *c*) Concave and convex tablets on dried dorsal valves, elevated above tension-cracked (tc), spherular (sp) primary layer, but also with tension-cracked, spherular coats; scale bars, 0.5 µm. (*d*, *f*) Concave tablets on the surface of a dried dorsal valve displaying well spaced nature; scale bars, 2 µm and 1 µm, respectively. (*e*) Concave tablet on dried dorsal valve with the coat split near the outer edge (oc) to expose contents of spherular apatite (sp); scale bar, 0.5 µm. (*g*) Imprints (it) on primary layer of dried ventral valve of completely removed or partly dislodged tablets (tt); scale bar, 1 µm. (*h–j*) Tablets treated with 0.2% bleach, and exposing spherular apatite (sp) between the outer (oc) and inner (ic) coats of partly digested tablets; scale bars, 0.5 µm, 200 nm and 0.5 µm, respectively.

XRD and EDX analyses indicate that only apatite or the contaminant halite could be the biomineral component of the tablets. Neither mineral assumes a rhombohedral or ditetragonal crystal structure, and these shapes are evidently fashioned during the intravesicular aggregation of the biomineral granules into tablets. The tablets are, therefore, assumed to be composed of protein and apatite and to form within the larval epithelium and then exocytosed onto the outer membranous pellicle. Following their emplacement, the edges of the plates become partly embedded in primary layer being secreted by the epithelium. In the earlier stages of their accumulation, the plates are probably flexible as their imprints indicate that they are mainly convex externally. After rupture of their membranous cover, however, many plates become concave externally (figure 8*f*). This change in convexity is probably an artefact resulting from the drying out of the dead shells. In any event tablets are rarely preserved on the larval surfaces of adult shells. Presumably they drift away as their pellicular cover degrades. (Postscript. The biomineral in the tablets is now known to be silica (see Williams *et al.* 1998*a*).)

(iv) *Canal systems*

Branching canals perforate the secondary layer of all discinid shells and complementary data have been obtained from *Discinisca* and *Discina*. In *Discinisca*, the canals, about 350 nm in diameter, are densely distributed (figure 10*a*) and frequently branch into parallel sets coalescing internally, with an average of 21 canal apertures in eight surveys, each of 100^2 µm, of a dorsal interior. TEMs of undecalcified shells (figure 10*d*) supplemented by scans of enzymic-digested interiors (figure 10*c*) reveal a mesh-like organic matrix in the vicinity of canals, assumed to be chitinous and proteinaceous. Galleries (figure 10*a*) and chambers of GAGs

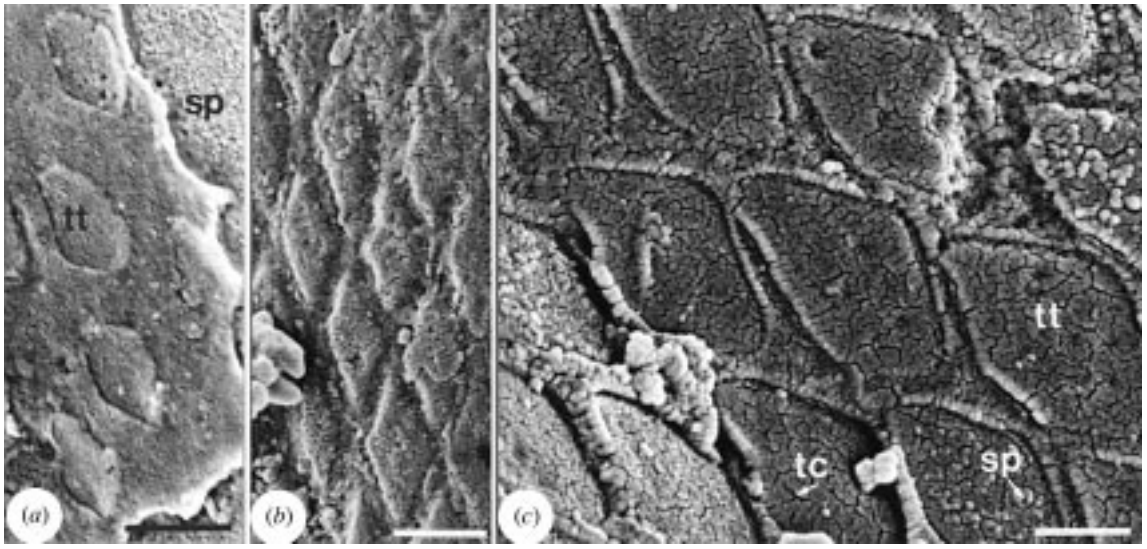

Figure 9. Scanning electron micrographs of the exteriors of discinid larval shells. (*a*) Tension-cracked fragment of the outermost coat of a dried valve of *Discina striata*, bearing imprints of tablets (tt) and underlain by a primary layer with spherular apatite (sp); scale bar, 1 µm. (*b*, *c*) Tablet imprints (tt) on the tension-cracked (tc), spherular (sp) external surface of the primary layer of *Pelagodiscus atlanticus*, treated with subtilisin; scale bars, 1 µm and 0.5 µm, respectively.

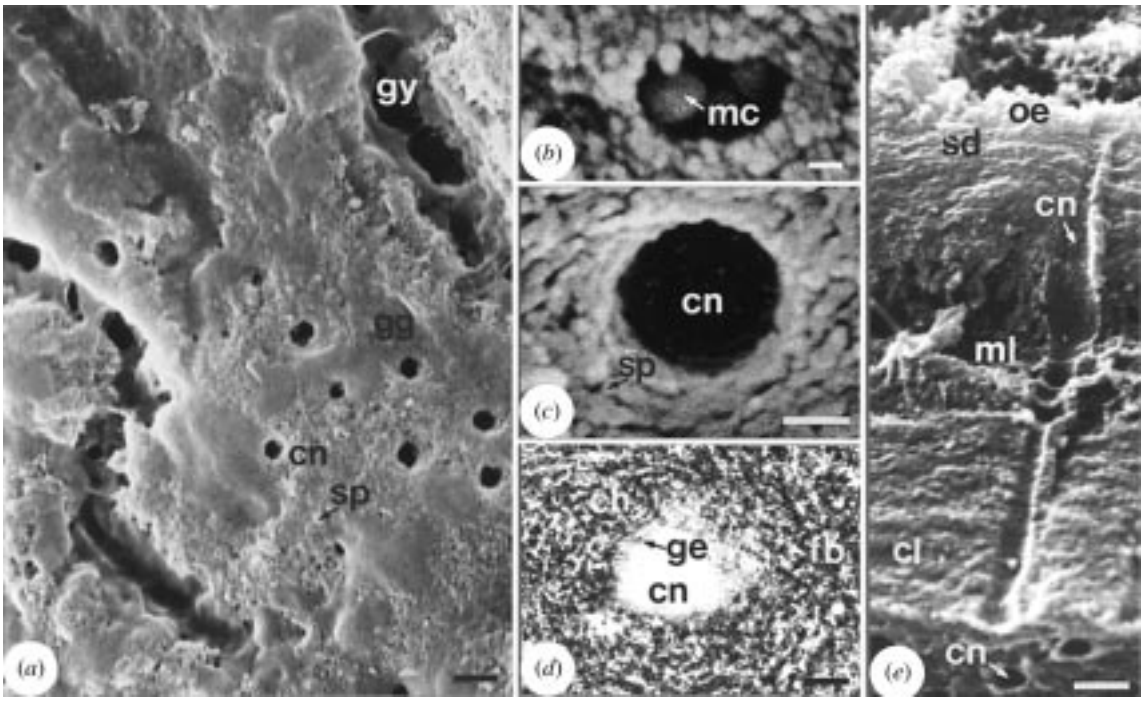

Figure 10. Scanning (*a–c*, *e*) and transmission (*d*) electron micrographs of sections and interiors of *Discinisca tenuis* (*a–d*) and *Discina striata* (*e*). (*a*) Internal surface of spherular apatite (sp) and GAGs (gg) showing canal openings (cn) and galleries (gy), treated with buffer; scale bar, 1 µm. (*b*) Detail of partly exposed chamber with mosaics (mc) in a critical point dried vertical fracture section; scale bar, 200 nm. (*c*, *d*) Cross-sections of canals (cn) on an internal surface treated with subtilisin and in a demineralized rubbly lamina showing spherules (sp) and granules (ge) of apatite associated with electron-dense and electron-lucent fibrils that are assumed to be 'actin' (fb) and chitin (ch), respectively; scale bars, 200 nm and 100 nm, respectively. (*e*) Critical point dried vertical fracture section of a succession of compact (cl) membranous (ml) and stratified (sd) laminae, secreted by outer epithelium (oe) and penetrated by a canal (cn); scale bar, 1 µm.

and concretions (figure 10*b*) are commonly enlarged around canal sets.

The best demonstration of differentiation of canal systems within the discinid shell has been in *Discina*. The wall and contents of a canal are secreted simultaneously with the laminar succession perforated by it. They are extruded from the same site on the apical plasmalemma (figure 11*a*,*b*) and can usually be traced through several laminar sets in a vertical section (figure 10*e*). The site of origin is marked by a lens of electron-dense fibrils and granules within a glycogen-rich cytosol, immediately beneath the apical plasmalemma and its overlying recumbent

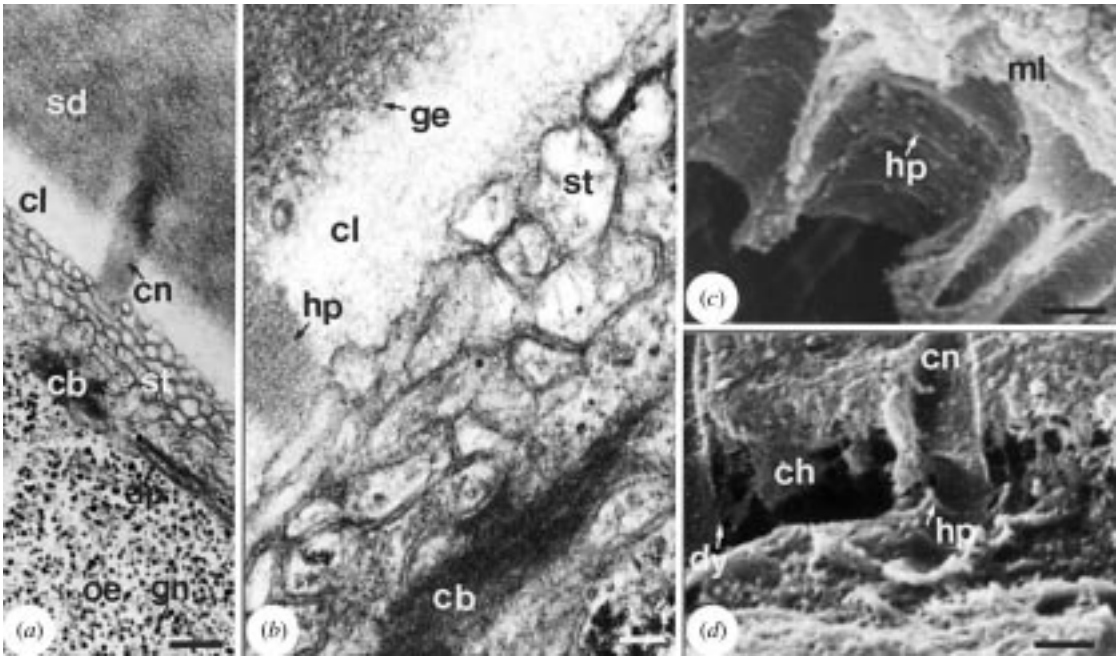

Figure 11. Transmission (*a*, *b*) and scanning (*c*, *d*) electron micrographs of canals in the shells of *Discinisca tenuis* (*a*, *b*) and *Discina striata* (*c*, *d*). (*a*) Demineralized section of integument, showing the relationship of a canal (cn) to a succession of stratified (sd) and compact (cl) laminae, the secreting tubular extensions (st) of the apical plasmalemma (ap) of outer epithelium (oe) rich in glycogen (gn), and the electron-dense fibrillar source (cb) of the canal; scale bar, 1 μm. (*b*) Detail of a hooped lining (hp) of a canal in relationship to a compact lamina (cl) with proteinaceous coated granules (ge), a zone of tubular extensions of the apical plasmalemma (st) and its source (cb); scale bar, 100 nm. (*c*) The hoop-like bands (hp) forming canal walls in a membranous lamina (ml); scale bar, 0.5 μm. (*d*) The widening and dichotomy (dy) of hooped canals (cn) within a membranous lamina with frayed sheets of chitin (ch); scale bar, 1 μm.

tubular extensions which may be up to five deep (figure 11*a*). The tubular extensions secreting the shell, contain electron-lucent particles and medium electron-dense fibrils (figure 11*b*). They show no signs of having been deflected by the canal, suggesting that they are more or less permanently arranged in a flexible ring above the secretory site of a canal on the apical plasmalemma.

A canal has two structural aspects dependent on the composition of the surrounding laminae. In a biomineralized succession, a canal is relatively narrow with a diameter of about 250 nm (figure 10*e*). Its membranous wall externally bears apatitic spherules and internally fibrils and rare spherules (figure 11*d*). The contents of a canal, as seen under the SEM, are also membrane-bound and divided into unequal segments by perforated transverse partitions.

In a predominantly organic succession, a canal rapidly widens to diameters of 750 nm or more (figures 10*e* and 11*d*). Its wall consists internally of hoops, less than 100 nm wide, and may bear rare spherules presumably of apatite (figure 11*b*,*c*). The hoops (figure 11*b*) comprise alternating bands of electron-lucent and darker beaded lineations which polymerize out of an exocytozed assemblage of particles (Williams *et al*. 1992, p. 99). The external surface of the wall supports a dense mesh and rarer strands linking canals (figure 11*d*), which are assumed to be chitinous and proteinaceous.

The inferred function of the homologous canal systems, permeating the shells of living lingulids and discinids, has to be compatible with several aspects of their origin and growth. These include: the initiation of canals on the outer surface of the outer mantle lobe and their persistence throughout shell growth; the synthesis of annulated canal walls from persistent lenses of electron-dense fibrous proteins just proximal of apical plasmalemmas of the outer epithelium; and the secretion of the canal system simultaneously with proteinaceous and chitinous networks pervading the shell (figure 12).

These characteristics suggest that canals serve as vertical struts interconnecting with the proteinaceous and chitinous nets to form an organic scaffolding in support of the stratiform successions of the shell. Indeed, laminar support appears to be the only feasible function. Unlike the large, papillose evaginations (caeca) of the mantle into the calcitic shells of punctate brachiopods, which serve as storage centres, no appropriate compounds have ever been found in canals. Only sporadic traces of shell constituents, degraded vesicular membranes and myelin figures, periodically sealed by transverse membranes (Williams *et al*. 1994, p. 252) have been identified.

(v) *Internal tubercles*

A unique feature of the *Discinisca* shell is a cluster of tubercles, each up to 200 μm in diameter and 50 μm high (figure 13*b*) on the posteriomedial part of the dorsal valve representing the body platform. The tubercles are surface expressions of dome-like cavities within the secondary layer (figure 13*a*), which form an irregular succession deep within the shell ('cedar-tree' structure). The entire complex consists of apatitic spherules, GAGs and membranes forming compact, rubbly and stratified laminae that differ from the rest of the shell only in their disposition.

Part exfoliation of a tuberculate cover reveals an underlying cavity containing a polygonal framework

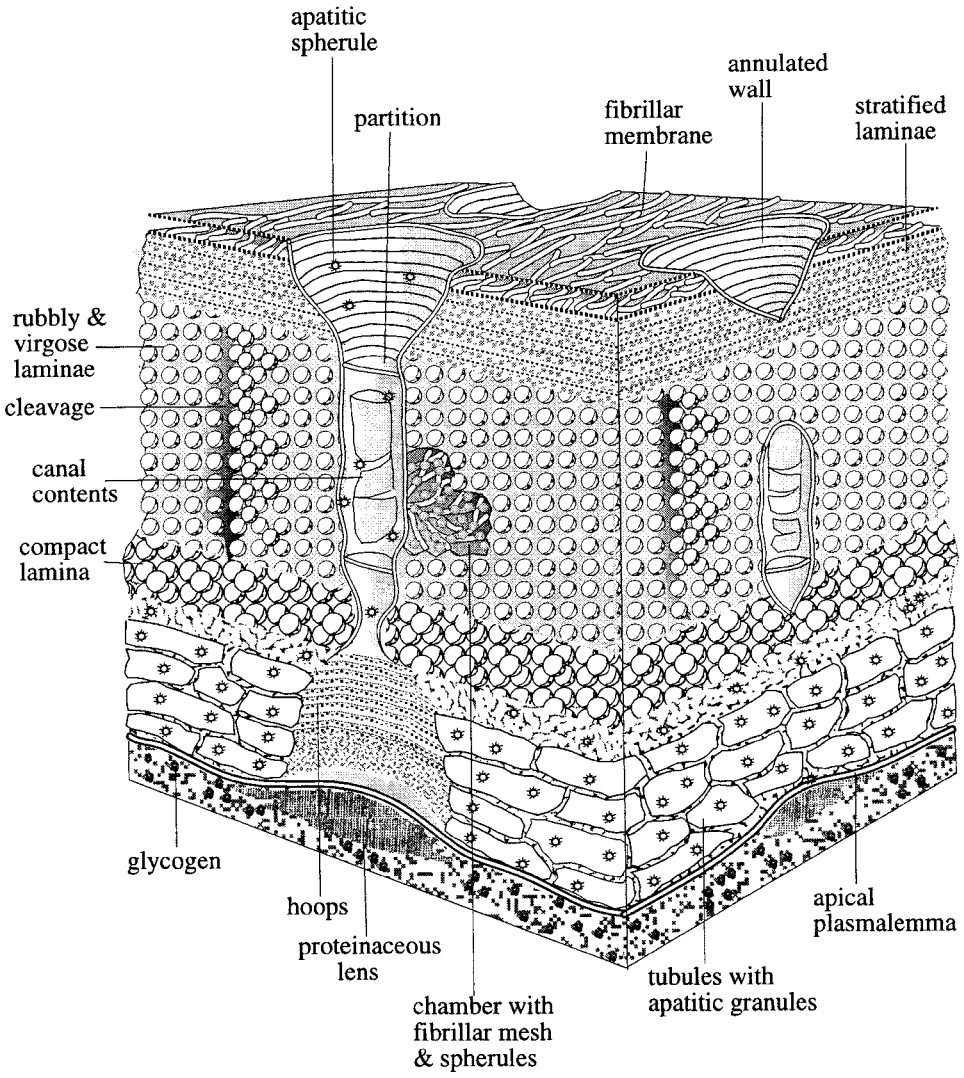

Figure 12. Stylized representation, at various magnifications, of the secretion of discinid and lingulid canals, and the main structural changes affecting them in different kinds of lamination.

varying from 13–30 µm in maximum diameter (figure 13*b*,*d*), with incomplete, vertical partitions. The polygons are occupied by membranes or radiating, apatitic wedges, a micron or so in maximum thickness (figure 13*d*), which are centripetal to a central aperture, normally occupied by a spherical or tuboidal body, about 3 µm across. The wedges are segregated into sectors of about 15° and bear traces of closely distributed fibrous proteins. In section, the central sphere or block (figure 13*a*,*b*) appears to be the top of a pillar in an outer dome, while the wedges and partitions are commonly pierced by oval apertures more than 2 µm in maximum diameter (figure 13*c*).

There is a close correlation between mature shell length (as an indicator of sexual maturity) and the presence of tubercles. It is therefore assumed that these tuberculate areas continually accommodate pockets of outer epithelium and connective tissue enclosing gonadal infolds (genital lamellae). In the breeding season, such pockets would develop within the secondary shell to contain gonadal lamellae and would then be sealed off by outer epithelial secretions at the end of the reproductive cycle. This would account for the presence below a tubercle of a 'cedar tree' arrangement of the dome-like cavities within the secondary shell, each representing a previous site occupied by pockets with gonadal lamellae.

(vi) *Formation of lamellae*

The growth of lamellae of *Discinisca* is a measure of the mobility of the outer mantle lobe relative to the shell margin and is relevant to understanding the development of concentric ridges (fila) characteristic of *Pelagodiscus* and all Palaeozoic discinids.

Lamellae, which may extend for a few millimetres beyond the general curvature of a valve, composed of periostracum and primary and outer secondary layers, all of which are easily distinguishable in back-scattered electron images (figure 14). On the outer surface of a lamella, the periostracum and primary layer form folds with wavelengths and amplitudes of up to 50 µm and 20 µm, respectively. These folds are not zones of contraction following the 'rupture' of the periostracum and primary layer at the edge of lamellae. They are rheomorphic structures induced by variations in the disposition of the outer mantle lobe and in the rate of shell secretion. Thus, immediately internal of a fold (figure 14*b*), a sequence of stratified laminae splits into two which diverge within the core of the fold to form a wedge with the primary layer coating the outer face of the fold. These wedges are filled with an organic mesh containing apatitic spherules, which was evidently deposited by an infra-marginal band of the outer mantle lobe simultaneously with the secretion of periostracum

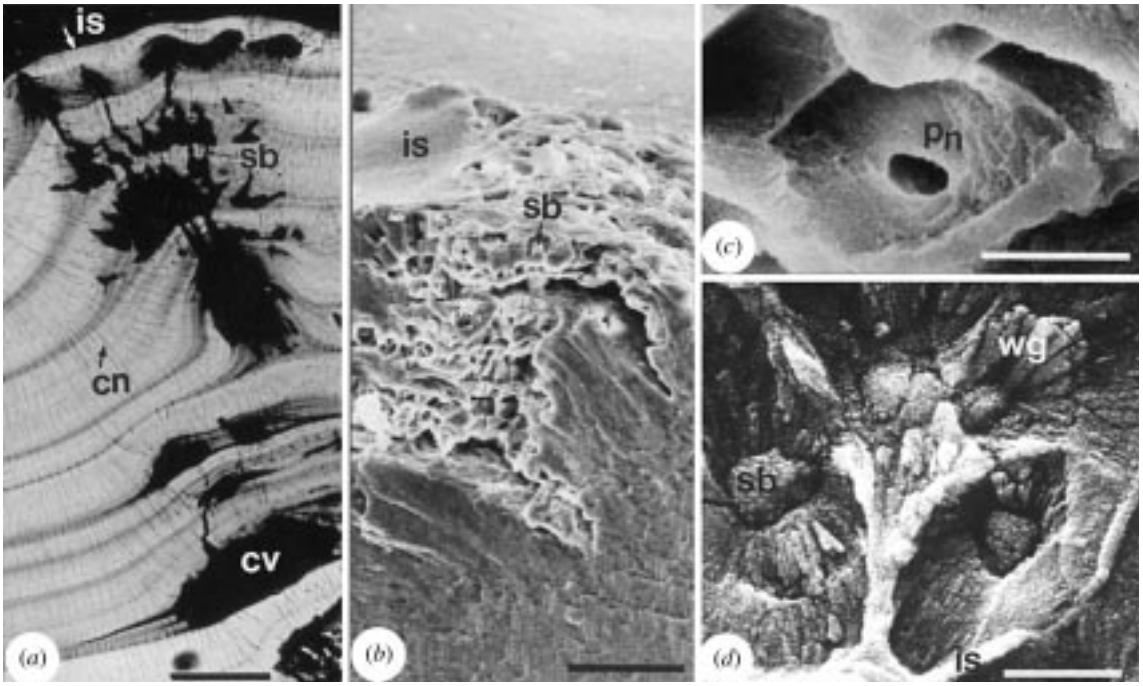

Figure 13. Scanning electron micrographs of internal tubercles in dorsal valves of *Discinisca tenuis* (*b–d*) and *D. lamellosa* (*a*). (*a*) Back-scattered electron micrograph of a polished, vertical resin-impregnated section of the secondary layer, treated with bleach, showing the 'cedar-tree' arrangement of cavities (cv) underlying the internal surface (is) of a tubercle within a canal-perforated (cn) sequence of laminae; scale bar, 50 μm. (*b*, *c*) Vertical fracture section, treated with proteinase-K, with a general view of cavities, some with exposed pillars forming spheroidal bodies (sb), beneath the internal surface (is) of a tubercle, and a detail of a perforated vertical partition (pn); scale bars, 50 μm and 5 μm, respectively. (*d*) Polygonal cavities immediately below the internal surface (is) of a tubercle with radiating wedges (wg) and spheroidal bodies (sb) treated with bleach; scale bar, 5 μm.

and primary layer at the tip of the lobe. The structures associated with these rheomorphic folds are the same as those of fila (compare figure 20*d* and *f*).

Several rheomorphic folds may develop before a lamella extension is terminated. The termination is marked by a sudden retraction of the mantle so that no periostracum nor primary layer are deposited along the edge or the inner surface of a lamella; and their secretion begins again only when they form the outer coat of the next lamella. This process of accelerated forward growth terminated by sudden retraction of the outer mantle lobe is very similar to that giving rise to lamellae in calcitic-shelled brachiopods (Williams 1971, p. 61), although no proteinaceous coats covering the inner surfaces of the *Discinisca* lamellae have yet been found.

(b) *Shell structure of other living discinids*

(i) Discina

The shell structure of the heavily mineralized *Discina striata* has already been described (Williams *et al.* 1992), but critical point dried fracture sections of the integument have provided new information, especially about membranous laminae. The rhythmic sets of the stratiform secondary layer typically consist of membranes or an organically rich stratified lamina succeeded inwardly by baculate and/or rubbly laminae grading into a compact lamina. The sheet-like membranes are normally accompanied by networks of fibrils with sporadic spherular apatite. These horizontal networks can give rise to sporadic strands trailing into apatitic laminae and are structurally indistinguishable from those found in *Discinisca* and *Lingula*.

(ii) Pelagodiscus

The outermost organic coat of the larval shell (see § 3a(iii) and the post-larval periostracum (Williams & Mackay 1979, p. 732) are essentially the same as those of *Discinisca* and *Discina*. The mature shell is likewise ornamented by capillae about 3 μm wide and increasing by dichotomy and intercalation (figure 15*a*,*g*). The sub-periostracal surface is sporadically pitted by shallow depressions, up to 2 μm in diameter (figure 15*g*), some radially arranged for short distances along capillae. They are assumed to be the casts of vesicles trapped beneath the periostracum.

The shell surface is additionally ornamented by concentric fila (figure 15*a*) with amplitudes of 20 μm or so, deformed by nick points and drapes, and anastomosing so that wavelength can vary from 15–25 μm. The fila vary in profile from parallel-sided to asymmetrical features, the crests of which may bulge laterally (figure 15*b*), almost to enclose interfilar troughs filled with the remains of planktonic and presumably indigenous micro-organisms (figure 15*a*). The variability of filar profiles is the result partly of creep during rheomorphic deformation but mainly of periodic outward deflections of the outer mantle lobe, followed by accelerated secretion as the lobe returns temporarily to a normal attitude. Consequently, secondary stratified laminae, filling in the fila, splay outwardly to terminate at varying angles to the interface with the retracted primary layer (figure 15*d*). These deflections are characteristic of the oldest discinoids and are most graphically displayed in the *Schizotreta* shell.

The secondary layer, immediately underlying a primary layer of evenly distributed apatitic spherules in a

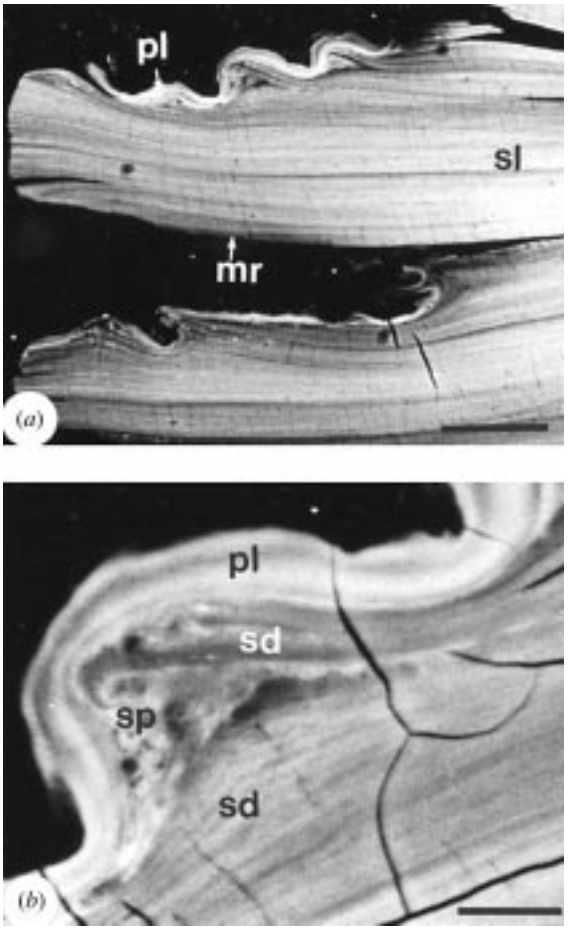

Figure 14. Back-scattered electron micrographs of a polished vertical resin-impregnated section, treated with bleach, showing concentric lamellae on the shell surface of *Discinisca lamellosa*. (*a*) General view of two lamellae with rheomorphic folding of the periostracum and primary layer (pl) relative to the secondary layer (sl) and the trace of mantle retraction (mr); scale bar, 50 µm. (*b*) Detail of rheomorphic fold showing the continuity of the periostracum and primary layer (pl), the divergence of stratified laminae (sd) at the steep outer face of the fold and the infill of spherular apatite in an organic mesh (sp); scale bar, 10 µm.

chitinous–GAG matrix (figure 15*a*), consists of stratified laminae (figure 15*b*,*d*). The main succession is composed of sets, typically 5 µm thick, with a sharp, external break, probably a proteinaceous membrane(s) as it can be digested by subtilisin, succeeded inwardly by a virgose lamina (figure 15*c*,*e*) (becoming incipiently baculate in the ventral body platform) grading into cleaved rubbly and spherular compact laminae (figure 15*e*).

Scars bearing epithelial imprints in the dorsal valve, which appears to lack the discinid canal system found in the ventral valve, support muscle bases divided into roots that are deeply embedded in galleries within the underlying shell. Mound-like impressions of cells on the ventral body platform, may bear a dense mat of fibrils (figure 15*f*) which are probably collagenous (compare Williams *et al*. 1994, fig. 43).

(c) *Shell structure of post-Palaeozoic fossil discinids*

Living *Discina* is distinguished from contemporary *Discinisca* by the part cementation to the substrate of the ventral valve but mainly by the morphology of the pedicle region; both genera, unlike *Pelagodiscus*, lack fila although all three are capillate. Chemico-structurally, *Discinisca* differs from *Discina* in the restriction of baculate lamination to the vicinity of the pedicle opening in mature ventral valves and the presence of tubercles in mature dorsal valves. A total of eight discinid samples of Jurassic and Eocene age were available for this study. All eight had previously been identified as *Discinisca* (seven specifically so), which accords with the traditional view that *Discina* has no fossil record. Chemico-structural data, however, are incompatible with this view; and have been used here for provisional generic identification pending a taxonomic revision of post-Palaeozoic discinids.

(i) *Tertiary discinids*

The shell of one of the three Eocene species identified by Muir-Wood as *Discinisca*, *D. insularis*, is too badly recrystallized to determine its structure; while the larval shell surface of a dorsal valve of another Lower Eocene species, *D. ferroviae*, has been obscured by varnish. In this valve, however, incipient baculi were found in the canaliculate secondary layer, associated with mosaics and irregular aggregates of spherular apatite (rubbly) inwardly of compact laminae as in *Discina*.

The dorsal valve of the third Tertiary species, the Middle Eocene *D. davisi*, is only 3 mm in diameter but is generally well preserved, except for the larval shell. Capillae (figure 16*a*) crossed by fine ridges that are probably remnants of the periostracum, cover the marginal costellae of the immature valve. The secondary layer is canaliculate and consists of well-developed lenticular baculate sets (figure 16*c*). A typical set begins with a sharply defined break followed by a zone of trellised baculi grading inwardly into a compact lamina. Recognizable patches of GAGs survive within the layer (figure 16*d*) and imprints of the outer epithelium are well preserved on the valve interior (figure 16*b*). It is likely that this species is also a *Discina*.

(ii) *Jurassic discinids*

The fine structure of the Jurassic discinid shells studied had mostly been destroyed by recrystallization, even that of specimens complete with setae, that had been immured by oyster shell overgrowth. Only the shell of one of three Early Jurassic species studied, *D. laevis*, showed possible traces of baculi as well as compact laminae in the ventral valve; those of *D. reflexa* and *D. holdeni* showed nothing more than stratiform lamination. The larval surface of *D. holdeni*, however, bore rhomboidal impressions resembling the imprints of tablets found on the larval shell of living discinids; and all three species have tentatively been assigned to *Discinisca*.

Both samples of undescribed discinids from the Upper Jurassic of Weymouth and South Ferriby were of immured, larval and immature shells. Both valves of both samples are 'baculate', with baculi 1.5 µm thick and orthogonally arranged (figure 16*g*). Assuming that these rod-like structures are baculi and not biomineralized canal walls, the abnormal thickening may be owing to recrystallization which, unusually, involves the accretion of spherulites up to 1.5 µm in diameter. The subprimary

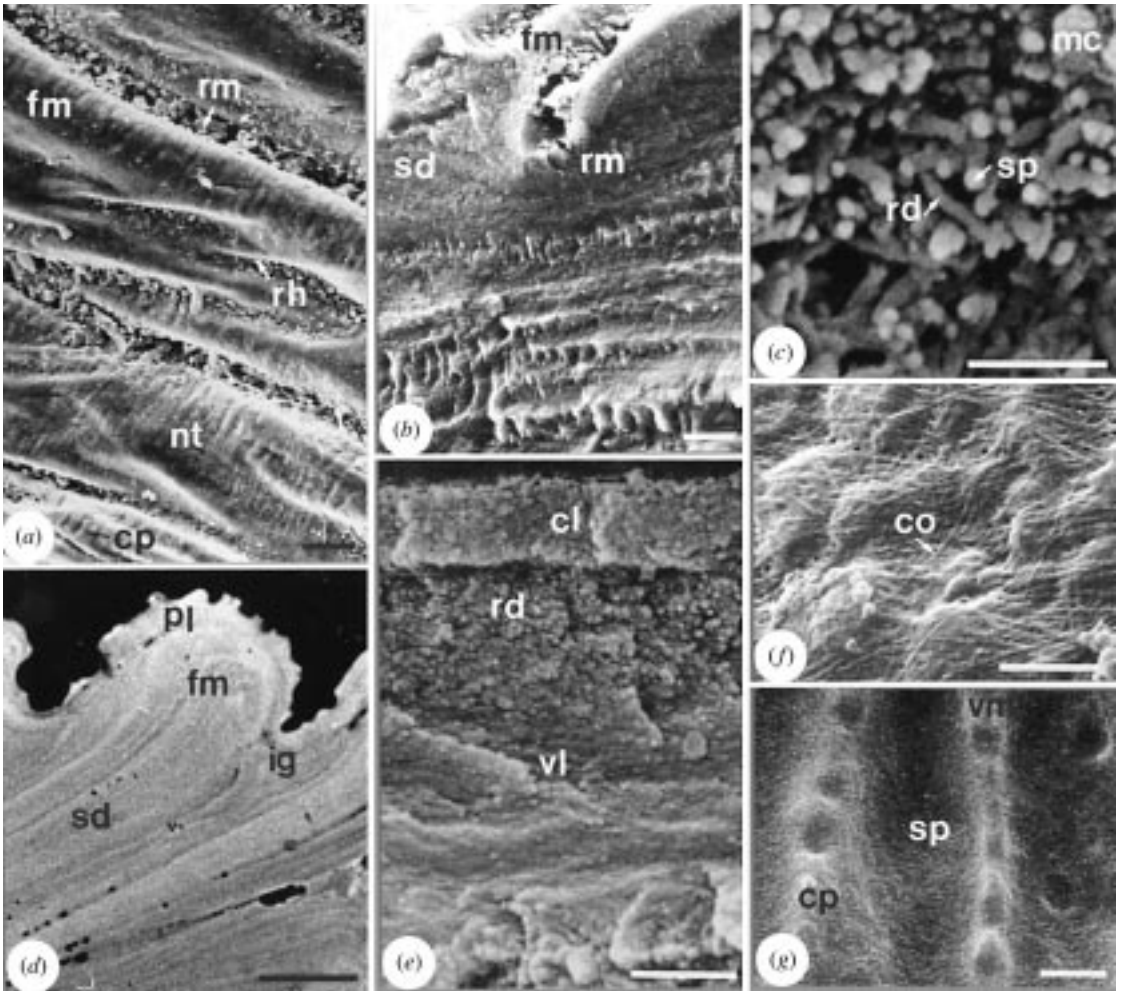

Figure 15. Scanning electron micrographs of the shell of *Pelagodiscus atlanticus*. (*a*) Exterior of dried dorsal valve with capillae (cp) and fila (fm) deformed by rheomorphic folding (rh) and nickpoints (nt) with remains of micro-organisms (rm) in interfilar spaces; scale bar, 50 µm. (*b*) Vertical fracture section of a dried valve showing fila (fm) almost enclosing troughs with remains of micro-organisms (rm) and a secondary layer of outer stratified laminae (sd) succeeded by laminar sets; scale bar, 25 µm. (*c*, *e*) Vertical fracture section treated with bleach, respectively showing rods (rd), mosaics (mc) and spherules (sp) of apatite in a virgose lamina (vl) and a typical set of virgose, rubbly and compact laminae; scale bars, 0.5 µm and 1 µm, respectively. (*d*) Back-scattered electron micrograph of a polished, vertical, resin-impregnated section of shell, treated with bleach, showing a filum (fm) composed of primary layer (pl) and secondary stratified laminae (sd) diverging at the interfilar groove (ig); scale bar, 25 µm. (*f*) Internal surface with a mat of fibrils identified as collagens (co); scale bar, 2.5 µm. (*g*) External surface of spherular (sp) primary layer with hemispherical imprints of vesicles (vm) aligned with capillae (cp); scale bar, 2 µm.

baculate set includes a variable thickness of rubbly apatitic aggregates grading inwardly into baculi capped by a compact lamina although the baculi of inner sets are usually subtended between compact laminae. A noteworthy feature of the South Ferriby sample is a regular pattern of flat, raised or indented rhombs with the major diagonal about 1.5 µm long (figure 16*e*,*f*). The rhombs are separated from one another by borders, about 200 nm wide, and are restricted to the larval shell surface and fade peripherally to the halo.

The Weymouth and South Ferriby samples are tentatively regarded as conspecific. The baculi in the dorsal valve and the rhomboidal pattern on the larval shell surface are characteristic of living *Discina* and the samples are provisionally assigned to that genus.

(d) *Shell structure of Palaeozoic discinoids*

A total of nine discinid and four trematid Palaeozoic genera have been described; seven of which have been studied although only two, *Orbiculoidea* and *Schizotreta*, were available in good samples. The shells in all samples are normally recrystallized but even nanometric original structures can be replaced pseudomorphously in well preserved valves. Membranes are represented by either narrow spaces or phosphatized sheets (figure 17*c*,*e*); organic infills, such as GAGs, by spaces (figure 17*d*) or mineral deposits especially apatite and calcite; and apatitic components by pseudomorphs varying in size from spherules, down to diameters of about 50 nm (figure 17*b*), to mosaics and rods at one micron or more (figure 17*c*).

(i) Orbiculoidea

The largest and best-preserved samples available for study were those of *O. nitida* from the Lower Carboniferous of Scotland and N. England. The chemico-structure of this species serves as a standard for the genus, although certain features of other *Orbiculoidea* are noteworthy.

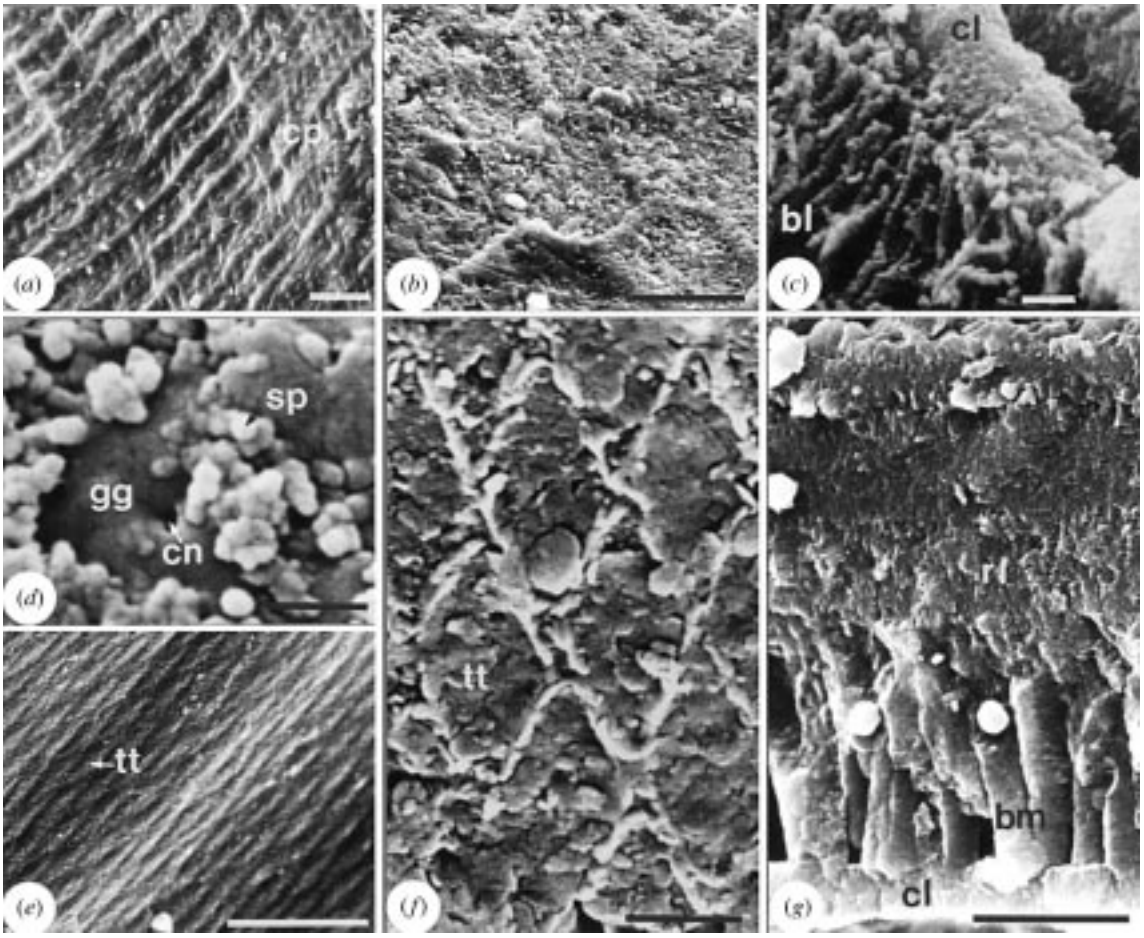

Figure 16. Scanning electron micrographs of post-Palaeozoic fossilized discinid shells. (*a–d*) Middle Eocene immature dorsal valve of *Discinisca davisi*: (*a*) external surface with capillae (cp), scale bar, 10 µm; (*b*) internal surface with hexagonal imprints of outer epithelium, scale bar, 10 µm; (*c*, *d*) baculate (bl) and compact (cl) laminae with fabric detail of apatitic spherules (sp), lithified GAGs (gg) and canal apertures (cn), scale bars, 1 µm and 0.5 µm, respectively. (*e–g*) Upper Jurassic *Discina*: (*e*, *f*) imprints of tablets (tt) on exterior of larval shell, scale bars, 5 µm and 1 µm, respectively; (*g*) orthogonal 'baculi' (bm) between compact (cl) and rubbly (rl) laminae, scale bar, 5 µm.

The primary shell of *O. nitida* is identifiable in back-scattered electron (BSE) micrographs as a layer between 5 and 10 µm thick. In SEM views it is seen as a vertically cleaved, spherular, patina-like coat (figure 17*a*,*b*).

The secondary layer is homologous with that of living discinids. In the umbonal areas, a fully developed unit of deposition (cf. figure 17*c*,*e*) appears to be a membrane(s) followed by: a stratified lamina with units between 300 and 700 nm thick, a rubbly lamina, up to 27 µm thick and occasionally cavernous with spherular rods and botryoids; and a baculate lamina, up to 30 µm thick, terminated by a cleaved, compact lamina of spherules and mosaics, normally less than 1 µm thick. Baculi are commonly preserved in various stages of collapse within a laminar chamber, but were apparently secreted as vertical or hexagonally disposed structures. They are composed of pinacoidal plates as well as spherules and prisms and rarely show any evidence of axial canals. Domes, representing aborted baculi, are densely distributed on the floors and ceilings of baculate chambers which also contain clusters of mosaics. Baculate laminae occur in both valves but are better developed in the umbonal areas of mature shells.

The main difference between the shells of *Orbiculoidea* and living discinids lies in the periostracum. The post-larval shell of *O. nitida* is ornamented by subcircular pits which are hemispherical or, rarely, flat-bottomed. The pits, which are commonly deformed into semi-ellipsoids, average 2.5–3 µm in diameter at 3–5 mm peripheral to the larval shell (Williams & Curry 1991). Pit distribution is normally graded in bands bound by concentric ridges (fila) about 25–40 µm wide and at intervals of 60–300 µm dependent on intercalations of impersistent fila (figure 18*a*). On the outer side of a filum and extending outwardly for about 30 µm, the pits are hexagonally close-packed. Beyond this zone the pits become aligned radially and segregated by strips of shell into single or double rows (figure 18*b*), 5–7 µm wide, although arrays, up to eight rows across, also occur.

The shell surface is seldom free of fine rheomorphic folding. Some interfilar surfaces may be rucked by concentric swarms of periclines, 7 µm or so in wavelength and sporadicaly intersected by nick points (figure 18*a*). Other sets include periclines with wavelengths of about 1 µm, which are themselves folded into narrow arcs with parallel sides, pointing outwardly and disposed about radially aligned pits (figure 18*b*). They have been interpreted as strain features induced in the periostracum and primary layer by setae (Williams & Curry 1991, p. 139).

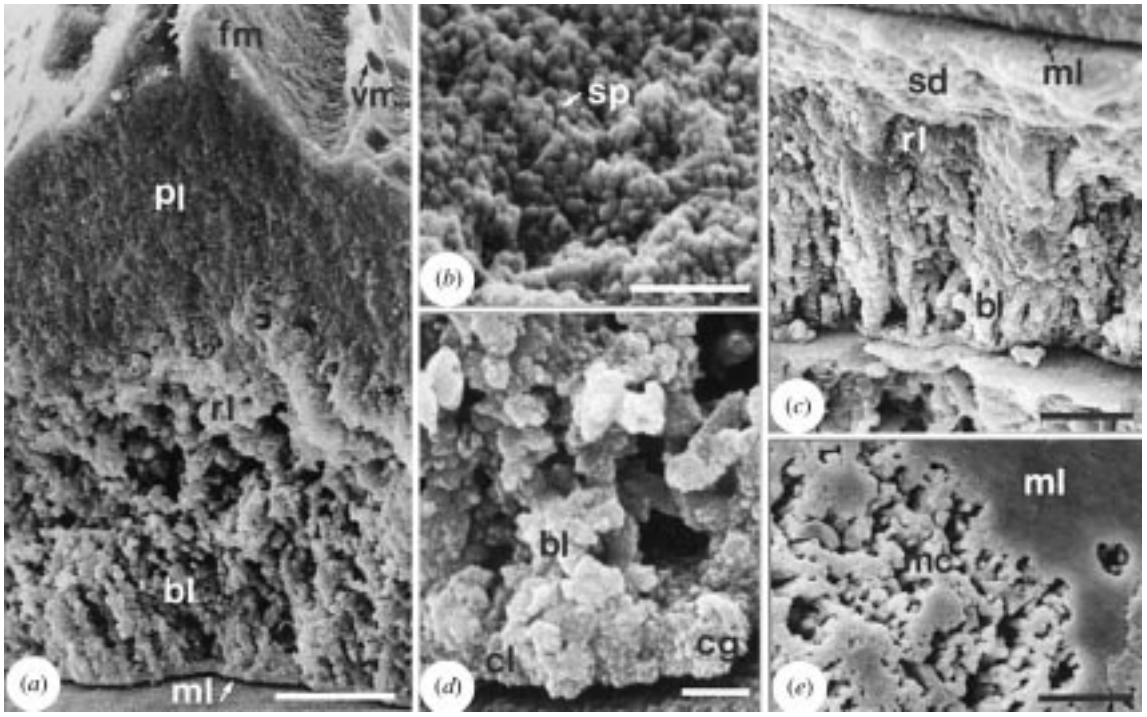

Figure 17. Scanning electron micrographs of the shell of the Carboniferous *Orbiculoidea nitida* from Reedsdale. (*a*, *b*, *d*) A vertical fracture section of shell with filum (fm) and a vesicular (vm) external surface showing the spherular (sp) primary layer and a secondary layer of rubbly (rl), baculate (bl) and cleaved (cg), compact (cl) laminae terminated by a break representing a degraded membranous lamina (ml); scale bars, 10 µm, 1 µm and 1 µm, respectively. (*c*) A typical set succeeding a membranous lamina (ml) consisting of stratified (sd), rubbly (rl) and baculate (bl) laminae; scale bar, 5 µm. (*e*) Vertical view of a set below the imprint of a membrane (ml) showing the labyrinthine arrangement of baculi with mosaics (mc); scale bar, 10 µm.

Pits are present everywhere on the shell surface, except for the strips segregating them into radial rows and along the crests of fila where they become shallow and die away to leave featureless patches. They were evidently hemispherical casts of bodies, preserved in a plastic substrate that was fine enough in texture to record nanometric strain features during phosphatization. The substrate is assumed to be homologous with the primary layer of living discinids and also to have been composed of spherular apatite in an organic matrix mainly of GAGs. The pits are, therefore, likely to have been part of the cast of the inner bounding surface of the *Orbiculoidea* periostracum and could have been impressed by hemispheroids or spheroids as both kinds of bodies occur at the surfaces of other organophosphatic-shelled brachiopods.

The bodies making the pits were not homogeneous but were composed of hexagonally close-packed spheroids (figure 18*d*), about 700 nm in diameter, which themselves appear to have been clusters of smaller vesicles. Such ordered packing suggests that the bodies consisting of spheroidal aggregates were also spheroidal and that the rims of the pits containing them, represented equatorial intersections with the interface between periostracum and primary layer. A good example of the toughness of the coats of these composite spheroidal bodies is shown in the shells of the Silurian *O. rugata* and of the Carboniferous *O. nitida* (figure 18*c*) and *Lindstroemella* (figure 18*f*). Judging from their excessively wrinkled surfaces, such shells probably dried out long enough to have caused dehydration of the GAGs of the primary layer prior to their burial and fossilization in lagoonal silts. Desiccation would have resulted in the contraction of the primary layer into rheomorphic folds radiating from close-packed pits which would have retained their hemispherical shape (figure 18*c*) even after degradation of their organic frame.

An immature shell, provisionally identified as *O. koninckii*, from the Permian of Co. Durham has been so severely recrystallized as to preserve no more than a stratified succession with ghosts of compact lamina. The post-larval, filar shell surface, however, is characteristically orbiculoideid being rheomorphically folded and indented with semi-ovoidal, compound pits distributed in close-packed zones or columns of variable length, up to three rows wide. Within 1–2 mm of the halo of the larval shell, the long axes of 75 pits average 3.7 µm, ranging from 2.4–6.4 µm.

The shell of a Carboniferous *Orbiculoidea* from Spain was partly chloritized and revealed only that the shell structure was stratiform with recognizable stratified lamination. The well-preserved shell surface had been greatly affected by rheomorphic folding with drapes in radial arrays although the vesicular pits generally retained a hemispherical shape. There are three Lower Palaeozoic species of *Orbiculoidea* which provide complementary data to those on the shells of the younger *O. nitida* and *O. koninckii*; specimens of the Devonian *O. mediorhenana* were too badly recrystallized to afford any chemico-structural information.

The shell of the type species of *Orbiculoidea*, the Middle Silurian *O. forbesi*, has superficial pits distributed in the same way as those of *O. nitida*. The pits are commonly hemi-ellipsoidal (long axes averaging 4 µm and ranging

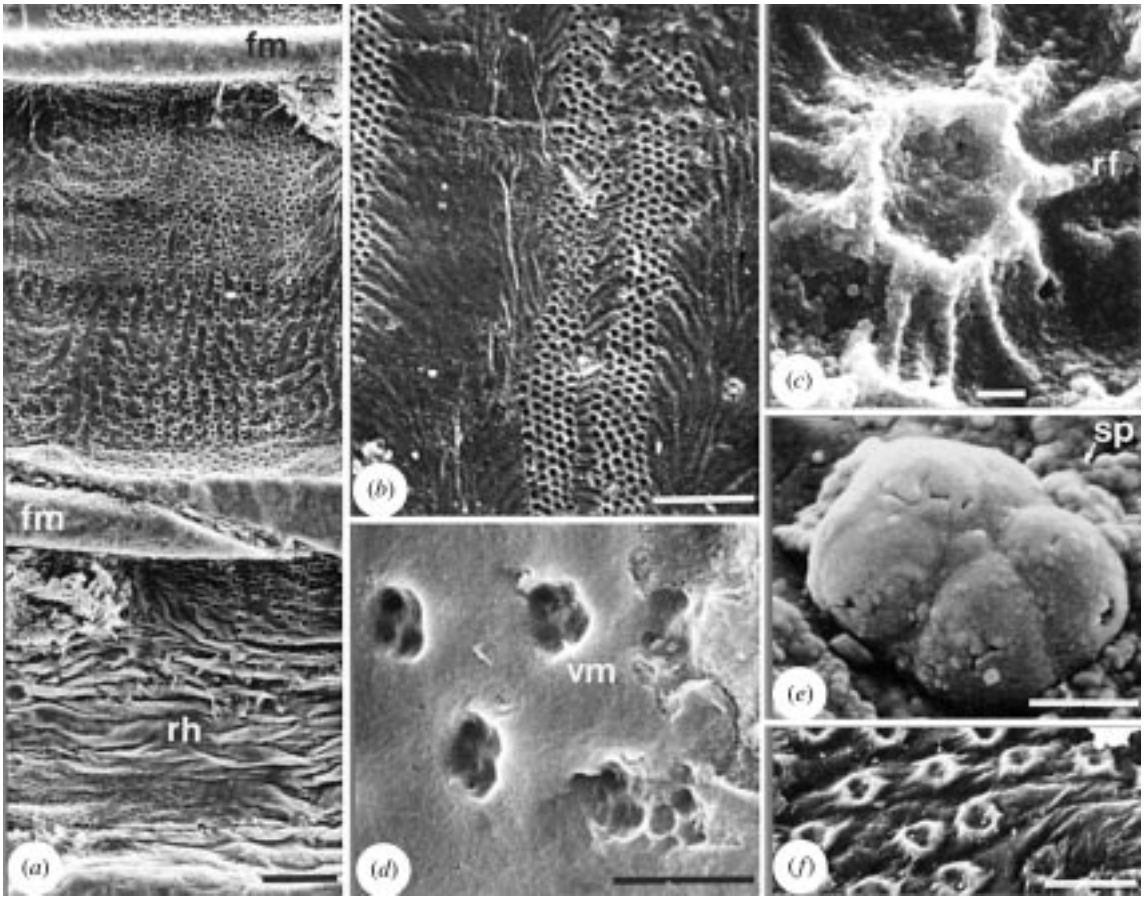

Figure 18. Scanning electron micrographs of the exteriors of shells of Late Palaeozoic discinoids. (*a–d*) Shells of Lower Carboniferous *Orbiculoidea nitida* from England and Blantyre, Scotland (*b*): (*a*) distribution of vesicular pits between two fila (fm) with an outer belt of rheomorphic folds (rh), scale bar, 50 μm; (*b–d*) details of trails of vesicular pits (vm) associated with rheomorphic folds, and of vesicular pits showing their composite nature and raised substrate with radiating folds (rf), scale bars, 20 μm, 1 μm and 5 μm, respectively, (*e*) Internal view of imprint of a composite vesicle in a spherular (sp) primary layer of *Roemerella*; scale bar, 1 μm. (*f*) Rheomorphically folded and pitted primary layer of *Lindstroemella*; scale bar, 10 μm.

from 2.4–5.8 μm in 66 counts), although rheomorphic folding of the primary layer appears to have been negligble; no compound pits were found. Fila are strong and bear the same relationship to baculate sets as those of *Schizotreta* to homologous lamination. In mature shells, body platforms, internal of the baculate secondary zone, are well developed as recrystallized laminae (figure 19*d*), up to 30 μm thick, with little evidence of their original fabric as seen in figure 19*b*.

The shell structure of the penecontemporaneous *O. rugata* is the same as that of *O. forbesi*. Surface pits are also not significantly different in size and distribution; and, with their raised rims surrounded by radiating rheomorphic folds, are indistinguishable from those found on some Scottish valves of *O. nitida*.

The shell of the Ordovician *O.* (?) *gibba* is typically orbiculoid in its filar surface, with pits in close-packed zones (figure 19*a*) periodically giving way to columnar arrays and averaging 4.3 μm (range 2.4–7.2 μm) in 15 estimates at 7 mm peripheral of the larval shell. There are, however, differences in shell structure and in the strength of development of surface lamellae.

The recrystallized primary layer (3–10 μm thick) is strongly developed and is succeeded by stratified laminae becoming virgose inwardly (figure 19*c*) as in *Discina* (Williams *et al*. 1992, p. 92). The underlying body platform is normally recrystallized into a massive succession, but laminar sets, about 30–40 μm thick, are discernible and usually consist of virgose or incipiently baculate zones bound by compact laminae.

The structural succession and growth of lamellose fila which are 300 μm or so in radial length, are revealed by the disposition of the lithified, pitted periostracum and its casts (figure 19*a*). The folded succession is asymmetric about a membranous lamina serving as an axial plane, with the stratified and virgose laminae of the secondary layer becoming attenuated along the inner flank of such a filum as a result of the relatively fast retraction of the secreting mantle lobe.

(ii) Schizotreta

The shell of *Schizotreta corrugata*, like that of some *Orbiculoidea*, consists of a primary layer, 8–15 μm thick, grading into secondary stratified laminae (figure 20*d*,*f*). The primary layer is composed of recrystallized granular apatite aggregated into spherules, 40–400 nm in diameter; and is likewise ornamented by pits and fila. The latter occur as concentric or impersistent arcuate ridges averaging 150 μm and 85 μm in wavelength and amplitude, respectively (figure 20*a*,*d*). The main differences

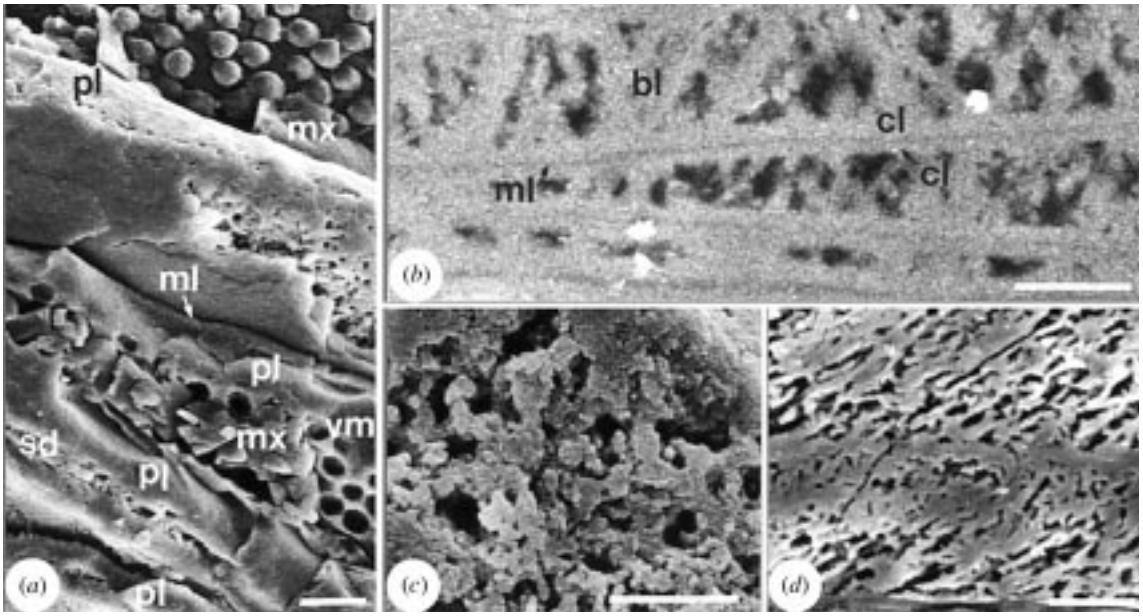

Figure 19. Scanning electron micrographs of the shells of Ordovician and Silurian *Orbiculoidea*. (*a*, *c*) Oblique and vertical views of a broken 'lamellose' filum at the margin of *O*. (?)*gibba* represented by an anticlinal fold between rock matrix (mx), with casts of vesicular pits, at the top of the micrograph and in the synclinal axis, in the lower part, delineated by vesicular pits (vm); the filum consists of primary layer (pl), stratified (sd) and virgose (seen as a labyrinth in (*c*)), membranous (ml) and thin, stratified laminae and primary layer; scale bars, 10 µm and 5 µm, respectively. (*b*, *d*) Vertical, polished sections of resin-impregnated shell of *O. forbesi*, treated with bleach: (*b*) back-scattered electron micrograph showing baculate sets of trellised baculi (bl), between compact laminae (cl) and separated by membranous laminae (ml), scale bar, 5 µm; (*d*) heavily recrystallized sets of the body platform; scale bar, 5 µm.

between the shells of the two genera are in the development of the surface pits and in the variety and sequencing of laminae.

The pits on the post-larval shell surface of *Schizotreta* are usually deformed into semi-ellipsoids with minor axes just under two-thirds the length of the major axes (figure 20*c*). They occur as close-packed bands (figure 20*a*) periodically giving way to radial columns, up to four pits wide, separated by strips without pits (figure 20*b*). These variations in pit distribution continue unchanged over the rounded crests of the fila but are affected in the interfilar troughs by rheomorphic folding which deformed the pits (figure 20*c*). The pits increased allometrically in size during shell growth. A distance of 1 mm from the larval halo, the major axes of 50 pits averaged 4.7 µm (range 3.8–7.3 µm) compared with 9.9 µm (5.2–13 µm) for pits 3.5–4 mm from the halo. Despite being almost three times as big as even more distal ones of *O. nitida*, the pits were not similarly composed of aggregates of small spheroidal bodies.

The secondary lamination of *Schizotreta* is dominantly membranous, compact and baculate (figure 20*d–g*). Stratified and rubbly laminae occur especially as subprimary successions (figure 20*d*,*f*), but the basic unit is a baculate set secreted at greatly differing rates medially (figure 20*e*) and marginally (figure 20*d*,*f*). *In vivo*, a set was composed of an outer membrane(s) succeeded inwardly by a compact lamina grading into a baculate zone capped by a second compact lamina. These laminae are now recrystallized although their original ultrastructure can be discerned. Thus, membranes are represented by a break in succession or a layer(s) of spherules, between 50 nm and 1 µm thick (figure 20*g*,*h*); compact laminae by apatitic prisms and rarer pinacoids with *c*-axes orthogonal to the plane of the set and between 400 nm and 1.5 µm thick (figure 20*h*); and baculate laminae by spaces of variable thicknesses criss-crossed by rods (figure 20*d–f*). In submedial successions where they are well developed, baculi are almost 530 nm thick (range 150 nm to 1.2 µm in 48 estimates). They consist of either irregularly stacked pinacoids (figure 20*j*) or better ordered prisms (figure 20*h*,*i*), both with *c*-axes parallel to baculum length. Both types have been found with central indentations suggestive of a non-mineralized core. A total of 50 readings of the inclinations of baculi to internal compact laminae averaged 65° (ranging from 30° to 90°) with acute angles more or less equally clockwise or anticlockwise.

Medially (figure 20*e*), a baculate set is seldom more than a few microns thick and the middle mineralized zone may be rubbly rather than baculate. The relatively slow secretion of the succession is confirmed by imprints of hexagonally packed epithelial cells, with long axes of about 18 µm, on the inner surfaces of compact laminae. The outer surfaces of compact laminae may also be mammillated, marking the sudden onset of apatitic secretion.

Marginally, towards the external shell surface where periodic development of fila could only have been effected by accelerations in shell secretion, successions of enlarged baculate sets trace the advance of outer mantle lobes relative to the main spread of the mantle. The plasticity of fila during their secretion has the same effect on their internal structure as rheomorphic folding (compare figure 14*b*).

A good example of this sequence of differential thickening is shown in young valves with a secondary layer of

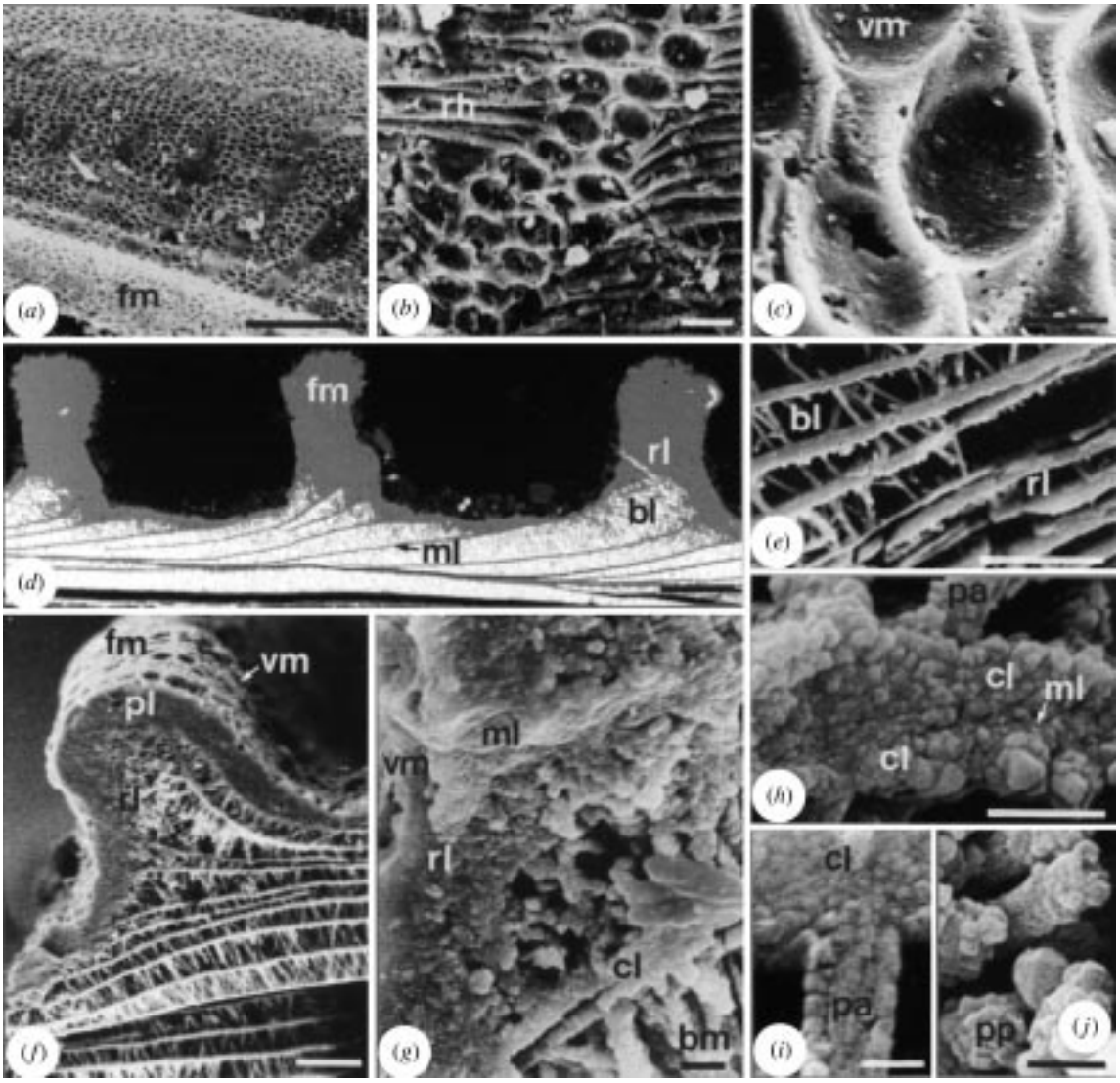

Figure 20. Scanning electron micrographs of the shell of *Schizotreta corrugata*. (*a–c*) The external surface with fila (fm) and arrays of vesicular pits (vm) affected by rheomorphic folding (rh); scale bars, 100 µm, 10 µm and 5 µm, respectively. (*d*) Back-scattered electron micrograph of a polished vertical section of a resin-impregnated shell showing the distribution of baculate (bl), compact and membranous (ml) and rubbly and stratified (rl) laminae bounded by the primary layer of fila (fm); scale bar, 50 µm. (*e–j*) Vertical fracture sections: (*e*) baculate (bl) and rubbly (rl) sets in medial part of shell, scale bar, 10 µm; (*f*, *g*) view and detail of sets of baculi (bm) compact (cl) and membranous (ml) laminae in relation to the primary layer (pl) and stratified and rubbly infill (rl) of fila (fm) with vesicular pits (vm), scale bars, 20 µm and 5 µm, respectively; (*h–j*) the junction between two baculate sets composed of recrystallized compact laminae (cl) and a trace of a membranous lamina (ml) and details of prismatic (pa) and pinacoid (pp) baculi, scale bars, 1 µm, 0.5 µm and 1 µm, respectively.

six or seven baculate sets (figure 20*d*). Along an interfilar floor in such shells, two or three membranes bounding baculate sets merge with the primary layer at about 25°. The inclination is comparable with that of the outer mantle lobe relative to smooth shell surfaces of living species. The secretion of a filum, on the other hand, can be effected only by an outer mantle lobe that was periodically deflected outwards. The splayed membranes within a filum (figure 20*d*,*f*,*g*) originated, more or less together, from an older membranous sequence about 100 µm posterior to the filum. The zone of origin apparently served as an axis, about which the deflected outer mantle lobe rotated during secretion of the filum. The most striking aspect of a filum growing in this way is the five- or six-fold increase in the cumulative thickness of the baculate and rubbly laminae at its core. In life, these wedge-like laminar sets would have consisted mainly of GAG infill.

(iii) *Shell structure of other fossil discinids*

Data from specimens of three Late Palaeozoic genera are scant but have confirmed the orbiculoideid affinities of two of them. The shells of the third genus, a Permian *Oehlertella* sp. were so coarsely recrystallized that only traces of a stratiform succession were preserved.

A total of two Carboniferous ventral valves, one of *Roemerella* and the other probably of *Lindstroemella*, had well-preserved surfaces of highly rheomorphic primary layers indented by compound pits with raised rims and radiating folds and averaging 2.7 µm and 3.5 µm, respectively (figure 18*e*,*f*). The spherular fabric of the primary layer of *Roemerella* (figure 18*e*) is probably closely

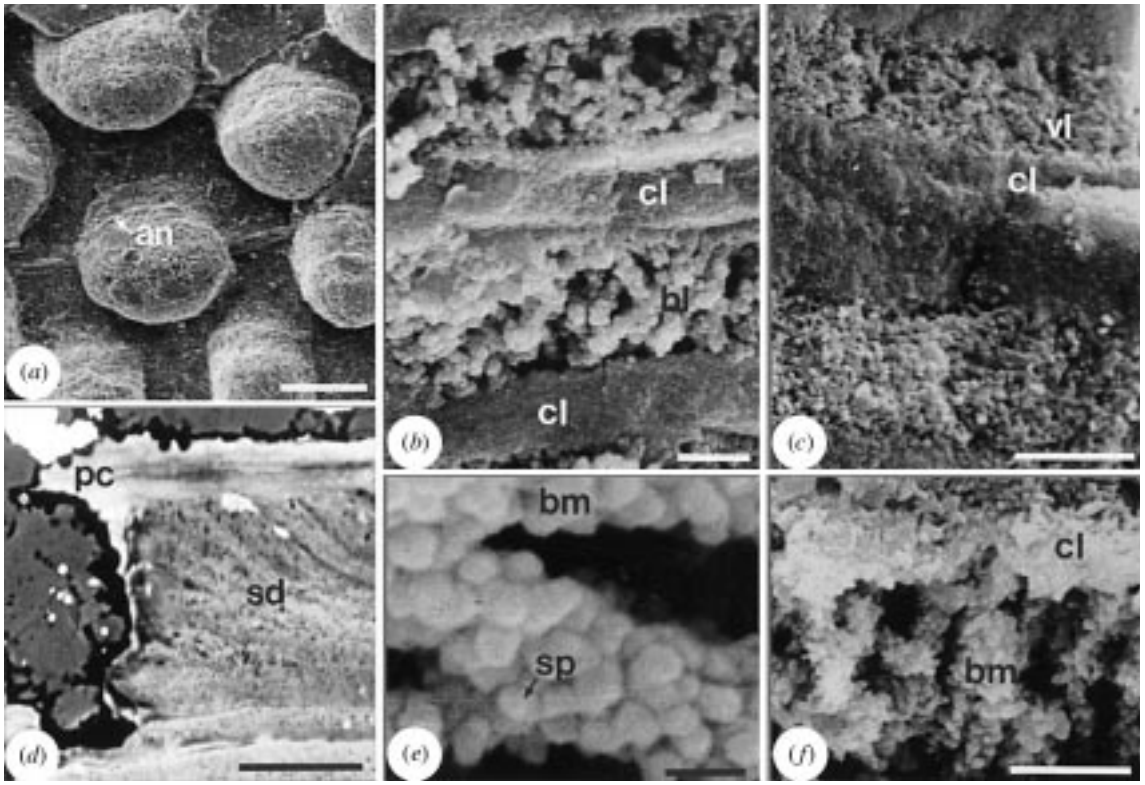

Figure 21. Scanning electron micrographs of trematid shells. (*a b*, *d*, *e*) The surface and sections of *Trematis millipunctata*: (*a*) internal view of the moulds of surface pits, with annulation (an), scale bar, 100 µm; (*b*, *e*) vertical fracture section of baculate sets of the secondary layer composed of trellised baculi (bl) between compact laminae (cl), with a detail of baculi (bm) composed of spherular apatite (sp), scale bars, 2 µm and 200 nm, respectively; (*d*) back-scattered electron micrograph of a polished, vertical, resin-impregnated section showing a pit constriction (pc) of primary layer and stratified laminae (sd) of the secondary layer, scale bar, 25 µm. (*c*, *f*) Vertical fracture sections of the secondary layer of *Schizocrania* showing sets of virgose (vl) and compact (cl) laminae, and a detail of incipient baculation (bm) in the body platform, scale bars, 5 µm and 2 µm, respectively.

comparable with the original state; while the secondary succession of both appears to have been dominated by laminar sets, up to 12 µm thick, with compact laminae bounding coarsely recrystallized layers passing into slot-like cavities towards the pedicle openings. These layers were presumably mainly organic, possibly baculate, in the living shell.

(e) *Shell structure of trematids*

The shells of two trematid brachiopods, *Trematis* and *Schizocrania*, were available for study. *Trematis* is ornamented by hemispherical pits, with constricted external openings (figure 21*a*,*d*) arranged radially or quincuncially (Wright 1981, p. 475) and increasing allometrically in diameter to 500 µm at the margins of mature shells. The primary layer varies in thickness between 10 and 14 µm, at the external surface between pits, and between 1 and 4 µm as pit linings (figure 21*d*). The variation is owing to accelerated shell secretion during pit formation and to rheomorphic folding which more strongly affected the primary layer between the pits than their linings where the folding occurs as low annulations (figure 21*a*).

Immediately underlying the primary layer, the secondary layer consists of stratified laminae, splayed outwardly at the posterior sectors of pits (figure 21*d*) where they may become botryoidal or rubbly. This disposition is like that of secondary laminae relative to fila in *Schizotreta*. The inner succession of the secondary layer consists of sets of compact laminae bounding trellised baculi (figure 21*e*) about 270 nm thick and subtending angles between 40° and 85°. The sets, 7–25 µm thick (figure 21*b*), are similar to those found in *Schizotreta*.

The radial ribs of *Schizocrania* are not homologous with capillae of living discinids. They are 15–20 µm thick and reflected undulations of the outer mantle lobes that possibly accommodated the proximal zones of the setal fringes. They are associated with rheomorphic drapes and nick points deforming the primary layer. Laminar sets of the secondary layer, which may be up to 10 µm thick, consist of compact and intercalated virgose laminae (figure 21*c*) with the latter becoming incipiently baculate within the body platform (figure 21*f*).

(f) *Chemistry of the discinoid shell*

Only a few data have been published on the chemistry of the organic and mineral constituents of discinoids (Jope 1965, p. H161). Indeed no attempt has previously been made to establish whether there are any significant biochemical differences between the shells of the living discinids and lingulids. The first part of this section is therefore devoted to biochemical comparisons of the organophosphatic shells of living species, in expectation that such data will eventually be useful in distinguishing between organic residues in the shells of extinct discinids

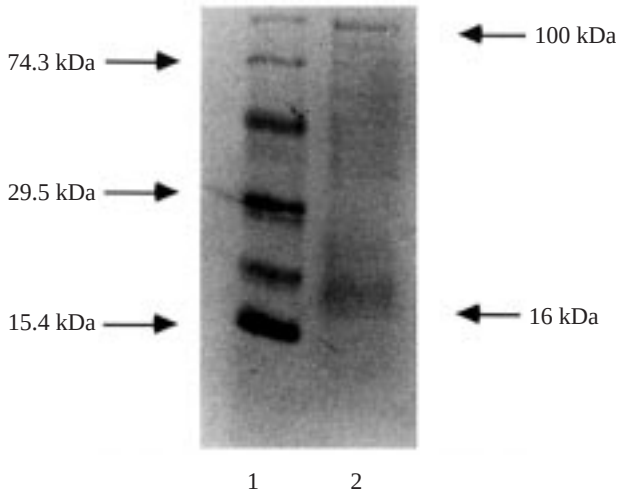

Figure 22. SDS-PAGE of mineral-associated proteins of *D. tenuis* shells (lane 2); EDTA-soluble proteins (equivalent to an extract from 1.1 g of shell) were fractionated in a 15% polyacrylamide gel alongside prestained proteins of known molecular weight (lane 1); proteins were revealed by staining with Coomassie Blue.

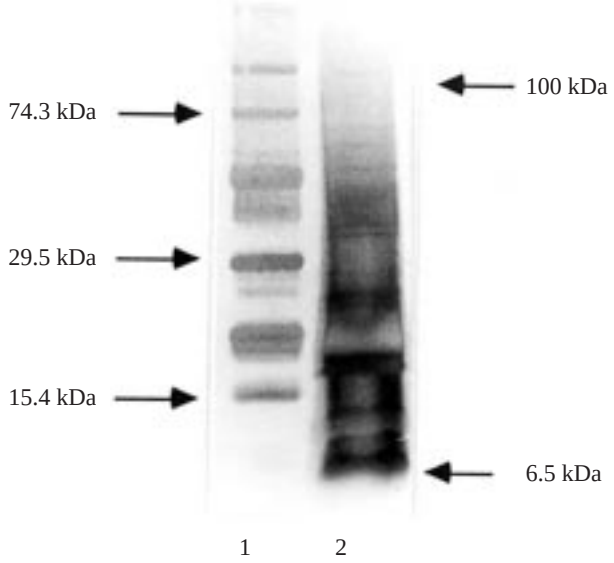

Figure 23. Silver staining of EDTA-soluble proteins of *D. tenuis* shells, fractionated by SDS-PAGE; proteins were stained with silver (Morrisey 1981) to reveal those proteins present at concentrations below the detection limit of Coomassie Blue; lanes (1) and (2) as in figure 22.

and the lingulids. The second part of this section reports the mineralogy and the biochemistry of 'intracrystalline' organic residues of fossilized discinoid shells.

(i) *Biochemistry of living discinid and lingulid shells*

The moisture content of the shells of *D. tenuis*, *D. lamellosa*, *D. striata*, *L. anatina* and *G. pyramidata* at 30% relative humidity is presented in table 1 along with the organic content as a percentage of the moist and dry weight. Lingulid shells, especially those of *G. pyramidata*, have the highest water content coinciding with the high concentration of organic material although the shell of *D. striata*, which has the lowest water content of these samples, also has a relatively high organic content.

The EDTA-soluble mineral-associated proteins of *D. tenuis* are presented in figure 22. The proteins were extracted (Williams *et al.* 1994) and fractionated on a 15% polyacrylamide gel (Schägger & Von Jagow 1987). Staining with Coomassie Blue reveals proteins in the molecular weight range of 16–100 kDa. Silver staining reveals more proteins and extends the lower range to 6.5 kDa (figure 23). At least one of the proteins, molecular weight 13 kDa, is glycosylated (figure 24), as determined by lectin binding using concanavalin A-peroxidase (Faye & Chrispeels 1985). The amino-acid composition of those proteins present in highest concentrations and that of the total EDTA-soluble extract is presented in table 2.

A total protein concentration of 55.9 pmol mg^{-1} shell was extracted by EDTA-dissolution of the shell. This represents only 0.016% of the total amino-acid content of the shell (see table 3). Most of the amino-acid content of the shell must be in the form of fibrous proteins which are insoluble under these conditions.

Amino-acid analysis did not distinguish between aspartic acid (D) and asparagine (N) or glutamic acid (E) and glutamine (Q) and the total values for D+N and E+Q are here assumed to be acidic amino acids. The level of acidic residues is higher in the larger proteins, with mole per cent values of 26 for the proteins of molecular weight 100 kDa and 72 kDa. Although there is no information regarding the conformation of these proteins *in vivo*, comparison of the ratio of acidic to basic amino-acid residues, may indicate the overall charge of these proteins. The ratio of acidic (D, N, E, Q) to basic (H, R, K) residues is 4.2:1, 4.7:1, 2.6:1, 4.8:1, 3.1:1 and 4.4:1 for the 100, 72, 48, 34, 21 and 16 kDa proteins, respectively. On this basis, the 34 kDa protein is the most acidic and the 48 kDa protein the most basic although isoelectric focusing is required to confirm this.

The total amino-acid composition of the shells of six discinid and lingulid brachiopods was determined by dissolving the shell with HCl (2N) and hydrolysing all proteinaceous material released; the results are presented in table 3. Of the discinoid brachiopods examined, *D. tenuis* contains the highest concentration of amino acids (350 nmol mg^{-1}) while *D. lamellosa*, *D. striata* and *P. atlanticus* contain 264, 257 and 218 nmol mg^{-1}, respectively. The valves of the discinoid brachiopods contain much higher levels of amino acids than the lingulids (*L. anatina*, 32 nmol mg^{-1}, and *G. pyramidata*, 44 nmol mg^{-1}).

The high level of organic material in lingulid shells relative to that of discinids (see table 1) is not reflected in the amino-acid content. The high water content in *L. anatina* and *G. pyramidata* shells suggests a more hydrophilic organic component such as chitin or GAGs. Indeed, both glucosamine and galactosamine were detected after HCl dissolution of valves of *L. anatina* and *G. pyramidata* as well as *D. striata*. Failure to detect these amino sugars in *D. tenuis* and *D. lamellosa* is attributed to the technique because amino sugars cannot be resolved from high levels of amino acids. It is, therefore, likely that dilution of the amino acids from *D. tenuis* and *D. lamellosa* dilutes the amino sugars below the detection threshold.

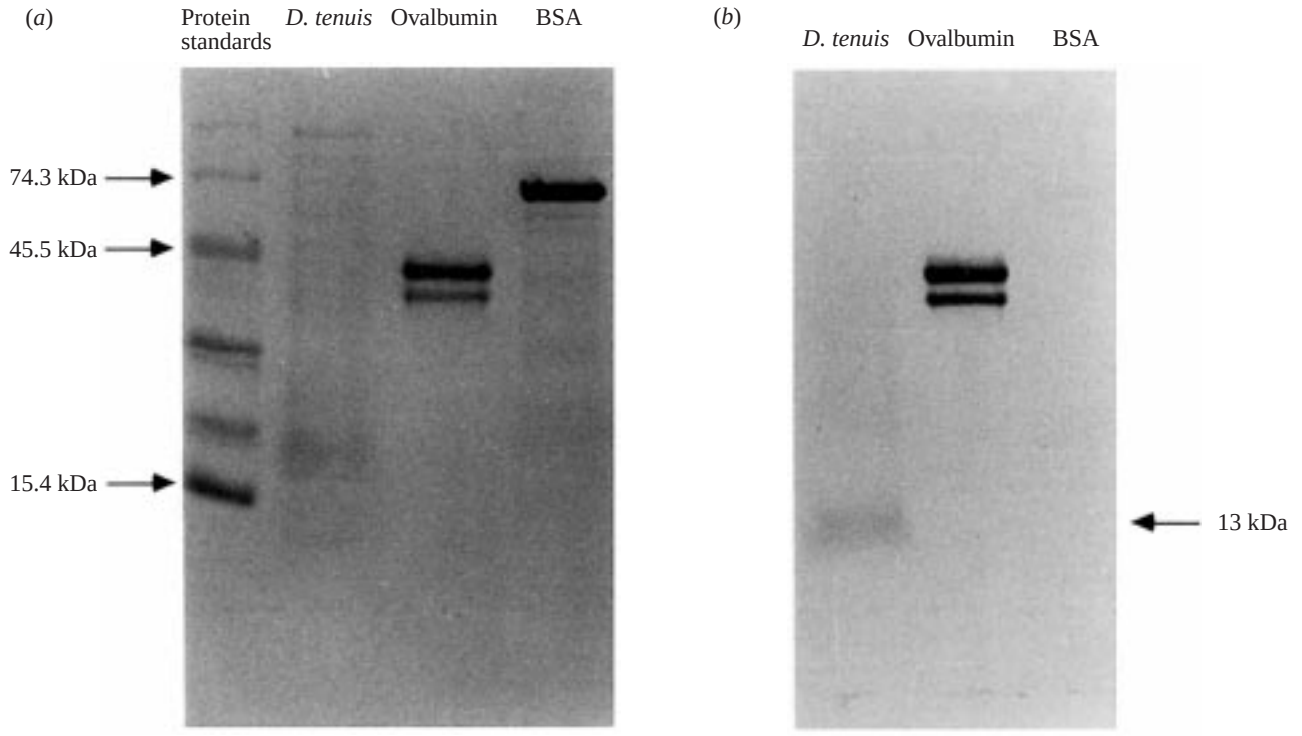

Figure 24. EDTA-soluble (glyco) proteins from *D. tenuis*. EDTA-soluble proteins of *D. tenuis* (equivalent to an extract from 1.1 g of shell) were fractionated on SDS-PAGE gels, as in figure 22, alongside proteins of known molecular weight and ovalbumin (3 µg), which is glycosylated, and bovine serum albumin (BSA) (5 µg), which is not; duplicate samples were applied to the gel and following electrophoresis, proteins were electroblotted onto a 'ProBlott' membrane and the membrane halved; one portion (*a*) was stained with Coomassie Blue to reveal all proteins present; (*b*) the membrane was treated with the lectin, concanavalin A, to detect glycoproteins.

Table 2. *Amino-acid composition (mole%) of the EDTA-soluble mineral-associated proteins of* Discinisca tenuis

amino acid	100 kDa	72 kDa	48 kDa	34 kDa	21 kDa	16 kDa	EDTA extract
D/N	15.1	14.9	11.9	11.2	10.2	10.8	16.1
E/Q	11.4	11.7	8.5	10.8	10.5	10.6	12.5
S	11.4	9.7	5.8	7.5	6.1	8.1	5.8
G	14.6	14.9	18.9	11.6	12.7	8.5	8.3
H	—	—	3.9	—	1.7	1.6	—
R	4.7	4.8	3.0	3.3	2.9	0.1	2.4
T	8.8	6.0	6.5	6.2	6.1	5.9	7.7
A	9.9	13.3	13.5	15.6	12.9	7.2	9.7
P	3.6	4.0	8.0	6.4	6.9	6.0	7.2
Y	—	—	—	1.1	0.9	2.3	1.6
V	5.7	2.4	3.7	5.2	4.2	5.6	6.9
M	—	3.6	3.5	2.1	2.3	3.6	1.5
C	0.5	—	—	—	0.4	6.2	0.6
I	4.7	5.2	4.8	6.3	6.7	5.6	5.0
L	6.2	6.4	5.0	7.3	8.1	7.4	6.7
F	3.1	3.6	3.5	4.6	4.9	7.3	4.8
K	1.6	0.8	0.8	1.3	2.1	3.1	3.3

As well as differences in the level of amino acids, with discinid shells containing higher concentrations than those of lingulids, some differences in amino-acid composition between discinid and lingulid shells are also apparent.

In the shells of living discinids, the average content of acidic amino acids (D–N and E–Q) is 14.5% with *P. atlanticus* containing the highest level (16.9%) and *D. tenuis* the lowest (11.9%). For the basic amino acids (H, R and K), the mean value is 13.2% with *P. atlanticus* containing the highest level (19.9%) and *D. tenuis* and *D. striata* the lowest with 9.7% and 9.8%, respectively. Glycine and alanine occur in large quantities. Glycine has an average value of 24.3%, with *D. tenuis* containing the highest concentration (31.6%) and *P. atlanticus* the lowest (8.8%). For alanine, the mean value is 22.7% and, in this case, *D. tenuis* contains the highest level (29.3%) and *D. lamellosa* the lowest (24%).

Table 3. *Amino-acid composition (mole %) and concentration of amino acids and amino sugars (glucosamine and galactosamine) in valves of six species of organophosphatic brachiopods*

amino acid	*D. tenuis*	*D. lamellosa*	*D. striata*	*P. atlanticus*	*L. anatina*	*G. pyramidata*
D–N	5.4	9.0	10.5	13.1	16.8	15.9
E–Q	6.5	4.2	5.6	3.8	6.5	2.9
S	4.3	4.9	2.5	6.3	4.2	3.5
G	31.6	27.0	30.0	8.8	16.3	23.0
H	—	0.2	—	0.7	0.7	—
R	8.6	12.0	8.7	18.5	4.9	6.7
T	3.6	3.5	3.1	14.2	4.4	2.7
A	29.3	24.0	28.0	9.6	22.9	23.0
P	4.6	6.2	5.1	7.9	8.0	6.4
Y	0.3	0.2	0.5	0.8	0.5	1.1
V	1.4	2.3	1.8	6.1	5.2	4.2
M	0.1	0.2	—	0.4	—	—
C	—	—	—	0.7	—	—
I	1.0	1.7	1.2	1.9	1.7	1.3
L	1.1	2.0	1.6	4.3	3.5	3.3
F	0.7	0.7	0.4	1.8	2.1	2.0
K	1.1	1.4	0.9	1.4	2.3	2.9
amino acids	350 ± 48	264 ± 35	257 ± 2	218 ± 7	32 ± 4	42 ± 8
glucosamine	—	—	0.3 ± 0.04	—	1.3 ± 0.2	2.3 ± 0.4
galactosamine (nmol mg^{-1})	—	—	0.09 ± 0.01	—	0.5 ± 0.07	0.8 ± 0.2

Table 4. *Amino acids* (pmol mg^{-1}) *extracted from fossil discinoid shells and, in some cases, associated substrate*

species	age	D–N	E–Q	S	G	T	A	Y	V	L	total
Discinisca davisi	Eocene	34	60	22	75	33	66	15	64	66	435
Discina sp.	Jurassic	142	10	3	33	—	9	2	2	2	203
oyster		41	2	1	21	—	8	4	3	4	84
Discinisca holdeni	Jurassic	127	—	13	22	—	5	3	4	—	174
Orbiculoidea nitida	Carboniferous	19	16	4	20	—	27	28	28	19	161
nodule		17	8	3	13	—	4	—	4	2	51
Orbiculoidea nitida	Carboniferous	23	39	12	107	2	20	10	25	26	264
Orbiculoidea forbesi	Silurian	18	4	1	13	—	3	6	3	6	54
matrix		23	0	8	7	—	—	5	2	—	45
Orbiculoidea rugata	Silurian	42	7	4	43	—	57	18	14	13	198
matrix		61	145	28	132	10	57	—	12	7	452
Orbiculoidea sp.	Silurian	2	3	8	38	2	9	5	3	6	76
Orbiculoidea sp.	Silurian	1	1	3	16	1	5	2	2	28	59
matrix		—	2	4	20	2	3	3	1	5	40
Orbiculoidea (?) *gibba*	Ordovician	5	5	6	51	17	24	2	8	20	140
matrix		5	2	3	7	—	1	2	—	—	20
Orbiculoidea (?) *gibba*	Ordovician	5	2	3	20	3	7	3	3	10	56
matrix		3	1	2	14	—	1	2	—	3	26
Orbiculoidea (?) *gibba*	Ordovician	1	3	7	30	2	9	4	3	9	68
Trematis millipunctata	Ordovician	2	1	6	40	9	9	6	2	11	86
matrix		—	—		13	3	3	2	—	6	29
Trematis millipunctata	Ordovician	2	3	4	24	3	10	3	4	11	64
Trematis millipunctata	Ordovician	8	23	30	110	5	37	28	31	49	321
Schizocrania	Ordovician	8	14	10	33	8	47	15	36	57	228
Schizotreta corrugata[a]	Ordovician	1	3	1	11	4	2	3	—	2	27

[a] Sample coated with varnish.

The shells of living lingulids contain higher levels of acidic amino acids than those of discinids, with an average value of 21.1%, and the levels of basic amino acids (H, R and K), with a mean of 9.1% which is lower than that of the discinids (13.2%). Glycine and alanine also occur at high levels in lingulids averaging 19.6% and 22.95%, respectively, although these are still lower than those in discinids.

(ii) *Mineralogy and biochemistry of fossilized discinoid shells*

A total of eight fossil discinoids were analysed by XRD using a Debye–Scherrer camera. They were the Palaeozoic *Orbiculoidea rugata*, *O. forbesi*, *O. nitida* and *Oehlertella* sp.; and the Mesozoic *Discinisca reflexa*, *D. laevis*, *D. holdeni* and a *Discina* sp. *Lingula anatina*, *Terebratulina retusa* and an inorganic calcite were also analysed to compare with the

fossil material as calcite (3.03 Å, 2.27 Å, 2.09 Å, 1.87 Å) occurs in *O. rugata* and *Oehlertella*.

A total of six diffraction lines (3.45–3.42 Å, 2.79–2.78 Å, 2.712.69 Å, 2.63–2.62 Å, 1.93 Å, 1.84–1.83 Å) representing apatite occur in seven of the fossil discinids (all except *D. holdeni* which is pyritized) and in *L. anatina*. A database search using the three main diffraction lines (3.45–3.42 Å, 2.79–2.78 Å and 2.71–2.69 Å), indicates a possible match with carbonate–hydroxylapatite (dahllite) and fluorapatite (francolite). Consideration of all diffraction lines (Å value and intensity) did not favour either dahllite or francolite. As dahllite and francolite are end members of a continuous spectrum of apatite compositions, it is likely that the fossil material lies somewhere between the two.

The Mesozoic and Palaeozoic discinids contain traces of the acidic amino acids (D–N and E–Q), as well as the aliphatic amino acids (S, G, T, A, Y, V and L) in various proportions (see table 4). A possible distinguishing feature is the relatively high level of D–N as in the Jurassic discinids, although the effects of fossilization and the lithification of entombing sediments on the proportions of amino acids surviving in shells have not been studied.

Biochemical comparisons with linguloid shells other than those of Recent species is presently not possible. Only shells of *Orbiculoidea nitida* and *Lingula squamiformis* from the same outcrop of the Ardross Shrimp Bed (Cusack & Williams 1996) have been analysed. Both samples were pyritized and their organic residues have been extensively degraded. However, the shells of three Early Cambrian paterinates from Australia and Sweden contained relatively high levels of aspartic acid (Williams *et al*. 1998*b*). The paterinates are the sister group of the lingulates and probably quite near the stem group of the phylum. The extreme antiquity and provenances of the paterinate samples suggest that some distinguishing features of integumentary amino-acid residues can be discerned even in the oldest of brachiopods.

4. CONCLUSIONS

Changes in the chemico-structure of living and extinct discinoid shells provide an insight into the evolution of an organophosphatic exoskeleton originating in Early Palaeozoic times. Some of the principal features of the living integument have been obscured or degraded during fossilization and their past nature has to be inferred. The canal system, for example, was frequently destroyed during diagenesis but is here regarded as having always been present (or possibly vestigial in one valve or another) because those of living discinoids and linguloids (Williams *et al*. 1994, p. 251) are identical (figure 12) and of the same dimension and disposition as those found in the acrotretide shell (Williams & Holmer 1992, p. 684). In contrast, other chemico-structural changes in fossilized shells are as well preserved as those morphological features that are traditionally used to decipher lingulate phylogeny. Accordingly, both chemico-structural and morphological transformations can be used in an analysis of discinoid phylogeny; and both kinds are listed in Appendix C(a). These data, therefore, afford an opportunity to compare discinoid phylogenies based on the morphology and the chemico-structure of the shell. However, many chemico-structural changes in fossilized shells have to be reconciled to the secretory regime of the living discinid integument before they can be meaningfully used in phylogenetic analysis. Such changes include transformations of surface features composed of a primary layer bearing imprints of the periostracum; and of the laminar successions of the secondary layer.

(a) *Transformations of periostracum and primary layer*

Rheomorphic folding of the periostracum and primary layer is strong in living discinids, even stronger in some species of *Orbiculoidea* and *Lindstroemella*, less so in *Schizotreta* and least so in the trematids. In living discinids, the folding is facilitated by the plastic nature of the organic constituents of the primary layer, especially GAGs, and the lack of an interconnected framework of apatite which occurs as dispersed spherules. It is concluded that the composition of the discinoid primary layer has always been much the same as it is today, except possibly for a reduction in the apatitic component in post-Silurian times.

The superficial pits of trematids and discinids are not homologous. Those of *Trematis* are casts of comparatively large (up to 500 µm in diameter) hollows that indented both periostracum and shell and were shaped by the entire outer mantle lobe. The discinid pits, on the other hand, range in average size from about 10 µm in *Schizotreta* to 3–4 µm in *Orbiculoidea* and other Late Palaeozoic genera and have been interpreted as imprints of periostracal spheroidal bodies on a primary layer as it was being secreted by the outer mantle lobe. Their precise origin is best considered in relation to the omnipresent basal layer of the periostracum.

The basal layer of the periostracum of all living brachiopods is secreted by vesicular cells on the inner surface of the outer mantle lobe. It acts as a substrate for any superstructures and/or infrastructures deposited by the inner epithelial (or lobate) cells and vesicular cells, respectively. It is unlikely that the spheroids were secreted infrastructurally, otherwise casts of them would have varied from spheroidal to flattened discoidal impressions as in acrotretoid larval shells (Williams & Curry 1991). More likely, the surface pits of mature Palaeozoic discinids are hemispherical casts of large spheroids secreted superstructurally by the inner epithelium of the inner mantle lobe at the periostracal grooves where the spheroids became joined to one another by the first deposits of the basal layer. The interfilar graded distribution is consistent with an initial exocytosis of spheroidal vesicles in close packs immediately outward of a filum, later reducing to radial trails secreted by a minority of inner epithelial cells in the periostracal groove, before all such vesicular exudation was temporarily supressed during an episode of accelerated secretion leading to the deposition of the next filum.

Speculation on the composition of a spheroid has to take into account evidence of a high surface tension that facilitated the cohesion of differently sized aggregates, and a tough coat enclosing a composite body that could become ellipsoidal without rupture during deformation of the primary layer. These considerations suggest that the spheroids, apart from those of *Schizotreta*, were originally composite vesicles, possibly of lipoproteins or mucins, with thick proteinaceous coats. Analogous vesicles with

proteinaceous coats, up to 100 nm thick, are secreted superstructurally by the lobate cells of living terebratelloids (Williams & Mackay 1979). Such a vesicular periostracum could, therefore, have been ancestral to the sheeted pellicular periostracum of living discinids, which is also secreted by the inner epithelium of the inner mantle lobe. Given this homology, the small vesicles that sporadically indent the primary layer of *Pelagodiscus* are secreted either by inner epithelium as bodies within a sheeted superstructure or by vesicular cells as droplets beneath the periostracal basal layer. Provisionally the *Pelagodiscus* vesicles are homologized with those forming the composite impressions on orbiculoideid shells.

The difference between pellicular (sheeted) and vesicular periostracal superstructures might have reflected the secretion of fibrillar glycoproteins and globular lipoproteins, respectively. A small transformation affecting the periostracal pellicular (sheeted) successions of living discinids was the growth of concentric scalloped ridges in *Discina* and *Discinisca* from a sheeted basement characteristic of *Pelagodiscus* (Williams & Mackay 1979, p. 732).

(b) *Transformations of the secondary layer*

The discinoid secondary layer has always been a stratiform succession of alternating laminae of predominantly organic and apatitic composition in a variety of textures, commonly arranged in ordered sequences and rhythmic sets. Thus the secondary layer of trematids, as well as discinids, normally consists of an outer, finely stratified sequence and inner sets of compact laminae separated by rubbly or cavernous virgose zones with residual mosaics and rods that presumably had once been immersed in GAGs with minor, dispersed apatite. Such sets are also well developed in Recent discinids and are likely to have been the standard units of secretion forming the ancestral secondary layer.

The development of baculi was the most conspicuous transformation affecting the ancestral secondary layer. It was linked with the growth of fila in the oldest known discinid, *Schizotreta*. Thus, baculi are exceptionally well developed in the marginal, wedge-like zones created by the accelerated shell secretion that gave rise to fila. These marginal baculate chambers are normally free of matrix, which suggests that, *in vivo*, baculi, supported by chitinous nets and proteinaceous strands, were immersed in GAGs containing only small amounts of dispersed apatitic spherules.

The typical baculate set of *Schizotreta* consists of a lithified membrane (or break) succeeded inwardly by a graded sequence of compact, baculate and compact laminae. This symmetrical cycle seems also to have been characteristic of *Orbiculoidea* (and the related *Lindstroemella* and *Roemerella*). However, in all three well-sampled species of *Orbiculoidea*, the Late Ordovician *O.* (?)*gibba* from Sweden, the Middle Silurian *O. forbesi* and the Early Carboniferous *O. nitida* from Britain, the outer biomineralized lamina tends to be variably stratified and rubbly as well as compact. Furthermore, baculi, which are as well developed medially as marginally, are commonly obscured by thick deposits of apatite. The differing sedimentary matrices and geological ages of these three samples suggests that these apatitic deposits were derived *in situ* from GAGs heavily charged with spherular apatite.

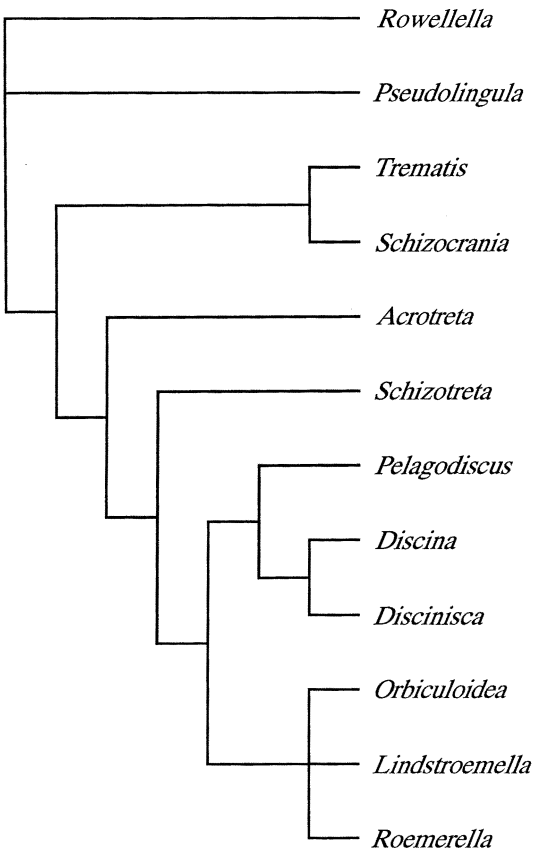

Figure 25. A majority-rule consensus of three trees derived by a branch-and-bound analysis of the matrix shown in Appendix C(b) with *Rowellella*, *Pseudolingula* and *Acrotreta* serving as outgroups; the only differences among rival trees are: *Schizotreta* becoming the sister group of the *Pelagodiscus–Discina–Discinisca* clade; and *Roemerella* emerging as the sister group of an *Orbiculoidea–Lindstroemella* clade.

Changes also affected the baculate sets of post-Palaeozoic discinid shells. The sequence within a typical set is a membranous and/or stratified lamina succeeded inwardly by baculi, supported by fibrous strands and nets in GAGs with minor, dispersed apatite, and capped by a compact lamina. In effect, the baculate sets of post-Palaeozoic genera were even more asymmetrically developed than those of *Orbiculoidea*, and with much smaller quantities of apatite within the GAG matrix. Furthermore, there is a difference in the distribution of baculate laminae which are best-developed medially within body platforms rather than marginally and are present in both valves only in *Discina*. In *Discinisca*, baculi are restricted to the ventral body platform and are only incipiently developed in the *Pelagodiscus* shell.

(c) *Phylogeny of the discinoid shell*

A phylogenetic analysis of transformations that effected the evolution of the discinoid shell was based on the chemico-sctructural and morphological features given in Appendix C(a). Character polarity was explored by the outgroup method as many structural features of the shell are found in organophosphatic species older than the earliest known discinoids. A recent phylogenetic analysis by Holmer & Popov (1996, p. 118) placed the paterulids

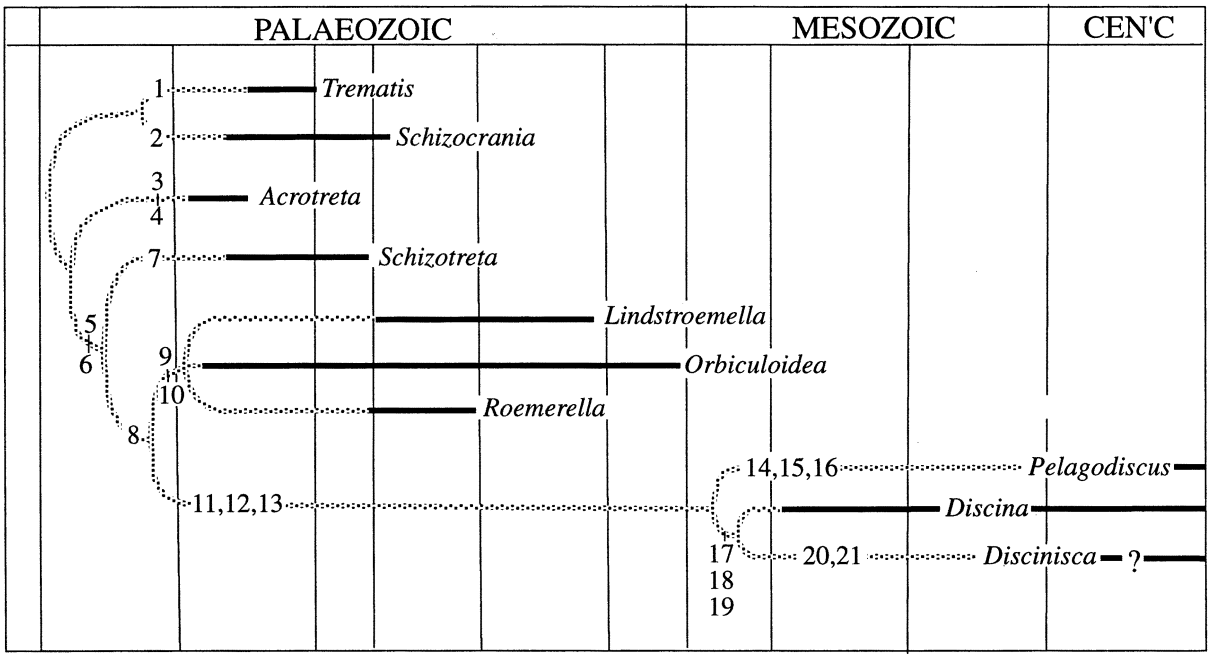

Figure 26. A phylogeny of nine discinoid genera and the acrotretoid *Acrotreta*, based on the cladogram of figure 25 superimposed on a geological chart with systemic boundaries spaced according to radiometric ages; the numbered transformations are as follows: 1, superficial pits; 2, incipient baculation only; 3, pitted larval shell; 4, baculation giving rise to camerate/columnar lamination; 5, baculate sets bounded by compact laminae; 6, subperiostracal vesiculation; 7, large, simple vesicles; 8, discinid baculate sets; 9, high concentrations of spherular apatite in the GAGs of baculate laminae; 10, composite vesicles; 11, tablets of larval shell; 12, capillae; 13, sheeted periostracum; 14, sporadic, simple vesicles; 15, loss of canals in dorsal valve; 16, incipient baculation only; 17, loss of vesicles; 18, loss of fila (replaced by lamellae); 19, development of scalloped, sheeted periostracum; 20, loss of dorsal baculation; 21, development of gonadal tubercles.

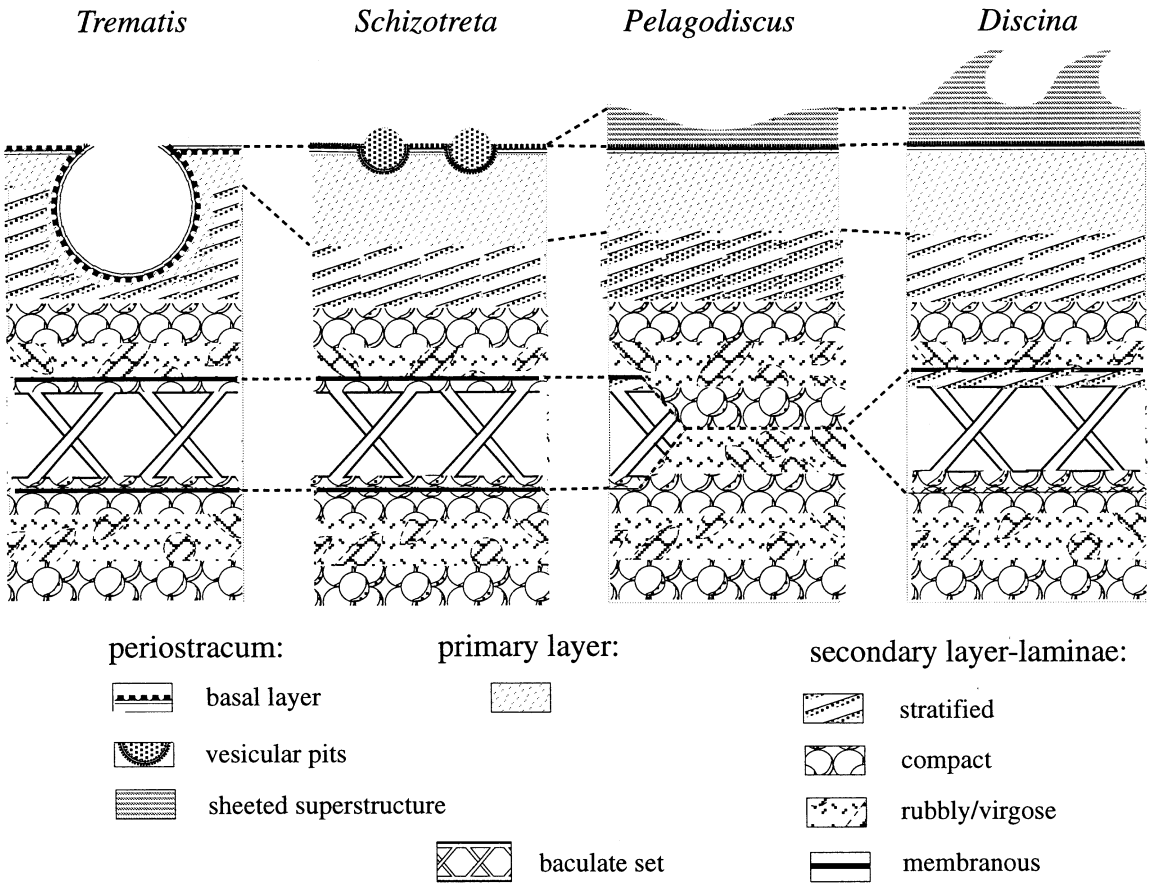

Figure 27. Correlation of stylized shell successions of four discinoid genera to show the differentiation of their periostraca and baculate sets superimposed on the basic structural arrangement of their primary and secondary layers.

as the sister group of a trematid–discinid clade within the lingulides. Mature shells of the linguloids, *Rowellella* and *Pseudolingula*, however, are respectively vesicular and baculate and were chosen instead of *Paterula* to represent the superfamily. Previously, the discinoids had been classified with the acrotretoids (Williams & Rowell 1965) and, as shells of the latter group are also characterized by such features as fila and baculi, the recently revised (Holmer & Popov 1994) genus, *Acrotreta*, was chosen as a third outgroup.

A branch and bound search, using the PAUP 3.1.1 program (Swofford & Begle 1993), found three trees with lengths of 79 steps and a retention index of 0.7. The strict consensus tree of these data is shown in figure 25 and a chronostratigraphic adaptation of it in figure 26. The most surprising taxonomic implication of the resultant relationships is the intercalation of acrotretids instead of the trematids as a sister group of the discinid clade. This transposition is only reversed when 16 characters, relating to the chemico-structure and growth of the shell, are excluded from the analysis. There is presently no reason for accepting such a selective use of character states. Even so, genealogies (figure 26) based on the cladogram shown in figure 25 are best regarded as provisional. The choice of outgroups has been influenced by the amount of information presently available on the shell structure of the preferred genera. When the structure of Early Palaeozoic organophosphatic shells is more comprehensively known, other stocks might be more appropriately used as outgroups and might give rise to genealogies more in keeping with the geological record. In particular, the use of a Cambrian lingulate, like the botsfordioid *Acrothele*, as an outgroup could change the cladistic relationship between the acrotretides and the discinoids.

A total of 21 noteworthy transformations have affected the shell of discinoids since their emergence in Ordovician times (figure 26). Some of these modify homoplastic morphological features. Imprints of hexagonally close-packed periostracal vesicles on shell surfaces, for example, are apparently polyphyletic, being characteristic of discinoids and the linguloid *Rowellella*. Yet the vesicles indenting the shell of the oldest discinoid, *Schizotreta*, are four or five times as large as those of *Rowellella* and probably differed in composition. The vesicles of *Schizotreta* could also have differed in composition from those of the closely related orbiculoideids, which were aggregates of membrane-bound secretion droplets that survived as sporadic, disaggregated bodies in living *Pelagodiscus*.

Other transformations modified symplesiomorphies such as baculate laminae. The ancestral baculate set (as typified in *Trematis*, *Schizotreta* and the 'columnar laminae' of *Acrotreta*) was a symmetrical sequence of compact, baculate and compact laminae. In descendant 'orbiculoideids', rubbly and virgose laminae partly replaced the outer compact lamina of the set. In living *Discina* and *Discinisca*, this asymmetrical set prevails and is even lost in the dorsal valve of the latter. A more profound reduction in baculation occurred independently in the trematid *Schizocrania* and the discinid *Pelagodiscus* although the incipient development of baculi in *Pelagodiscus* might be related to the small size of its adult shells. In contrast to symplesiomorphies like baculation and fila, several other structures were well-differentiated synapomorphies, notably the intravesicular secretion of tablets of protein and silica and their exocytosis to form a particulate biomineralized coat to the larvae of post-Palaeozoic discinids.

This research would not have been possible without the receipt of much material for chemico-structural analysis. The main gifts of specimens came from: S. Long and H. Brunton of the Natural History Museum of London; N. Clark of the Hunterian Museum of Glasgow University; J. Castilla of the Catholic University of Chile; C. Nielsen of the University of Copenhagen; L. Holmer of the University of Uppsala; T. Dutro and J. Thompson of the Smithsonian Institution, Washington, DC; J. Kallmeyer of Centerville, Ohio; M. Bassett and colleagues of the National Museum of Wales; and with B. Oelefsen of the Ministry of Fisheries and Marine Resources and G. Cloete and F. Botes of the Marine Centre at Swakopmund, Namibia providing facilities and assistance to A.W. for collecting *Discinisca tenuis*. Specimens, advice and access to localities were also generously given by: J. Bell of Durham; G. Biernat of the Palaeontological Institute, Warsaw; C. Burton of the University of Glasgow; P. Bouchet of the Muséum National D'histoire Naturelle of Paris; I. R. Congreve of Durham; P. G. Davis of Tamworth; C. Emig of the Centre d'Océanologie, Marseille; C. H. Holland of Trinity College, Dublin; N. Hollingsworth of NERC; S. Mackay of the University of Glasgow; D. Mackenzie of the Dunstaffnage Marine Laboratory, Oban; S. G. McLean of the Hancock Museum, Newcastle; M. Manceñido of the Natural Sciences Museum, La Plata; R. T. Paine of the University of Washington, Seattle; E. J. Polson of the University of Paisley; A. Rogerson of the University Marine Biological Station, Millport; R. Scott of the Scottish University Research and Reactor Centre, East Kilbride; W. H. Südkamp of Duitsland; P. D. Taylor of the Natural History Museum, London; E. Thomsen of the Tromsoe Museum; F. Whitham of Hull; C. Winkler Prinz of the National Natural History Museum, Leiden; A. D. Wright of the Queen's University, Belfast. Technical assistance of the highest quality has been readily given throughout the investigations by P. Ainsworth, D. Gourlay, D. McLean, S. McCormack, R. MacDonald, M. McLeod and D. Turner of the University of Glasgow, and by M. Corrigan of the University of Paisley. Work in the laboratory and the field has been fully supported by grants from the NERC (GR3/09604 and GR9/02038) and the Royal Society (RSRA/C.027 for M.C. and RSSQG 16604 and the Browne, Hill and Murray Research Funds for A.W.). We are indebted to all those colleagues and funding bodies listed, and many more besides, for such comprehensive support of the project.

APPENDIX A. MATERIALS

The shells of 27 species of discinoid brachiopods, belonging to ten genera and ranging in age from the Ordovician to the present day (figure 28) have been investigated chemico-structurally. Fossils were preserved in a variety of sedimentary rocks; their taxonomic identification and provenance are given. Specimens dissolved out of rock by 5–10% acetic acid are in bold face. The order of listing is generic–stratigraphic and those still accessible in museums are prefixed thus: BM(NH) (Natural History Museum); GLAHM (Hunterian Museum); and NMW (National Museum of Wales). The relative ages of samples are shown in figure 28 by the numbers accorded the species, as follows.

1. *Trematis norvegica* Cocks, Ordovician (Ashgill), Hoverdoya, N. Oslo, Norway; NHM BB76080, BB76086, BB91666.
2. *Trematis millipunctata* Hall, Upper Ordovician (Caradoc to Ashgill):

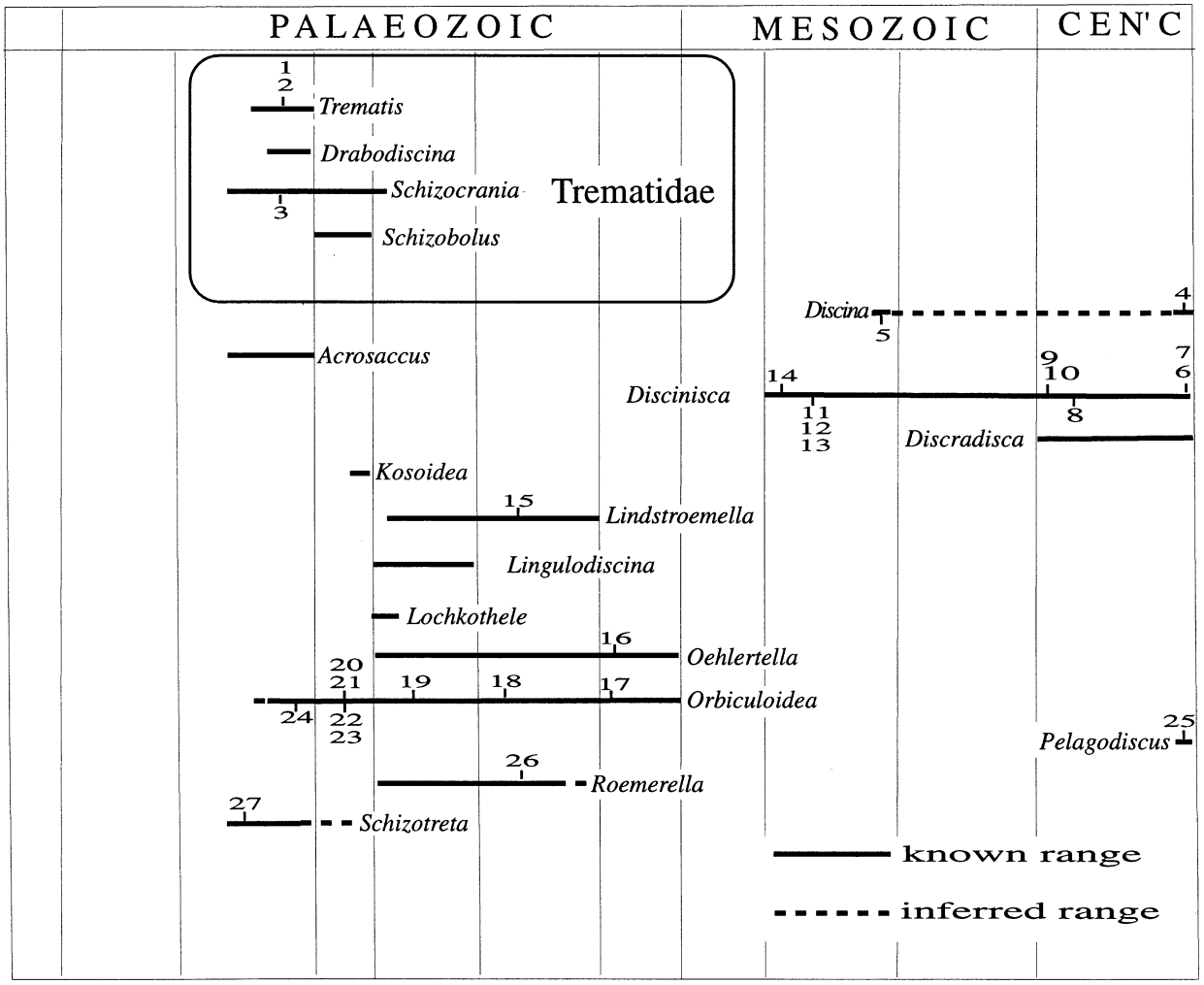

Figure 28. A geological chart, with systemic boundaries spaced according to their radiometric ages, showing the chronostratigraphic ranges of the 17 genera assigned to the Discinoidea, and the distribution of the 27 samples of the ten genera used in this investigation; the names, geological horizons and localities of the numbered species are given in Appendix A.

(*a*) Richmondian, Waynesville Formation, Causeway Road (Fairfield Road), 0.25 miles west of bridge crossing Brookville Lake, IN, USA; **GLAHM 101473–101474**.
(*b*) Maysvillian, Corryville Formation, Florence (38°59′4″ N, 84°37′45″ W), KY, USA; GLAHM 101484.
(*c*) Edenian, Kope Formation, excavated hillside by Kentucky State Route 17 (39°2′16″ N, 84°31′54″ W), KY, USA; GLAHM 101483.
(*d*) Unknown localities (Ohio/Kentucky/Indiana area, USA); GLAHM 101475–101482.

3. *Schizocrania filosa* (Hall), Upper Ordovician (Ashgill):
(*a*) Maysvillian, Corryville/Bellvue Formations, Ohio State Route 125, west of Georgetown, OH, USA; GLAHM 101485–101490.
(*b*) Maysvillian, Corryville/Bellvue Formations, US Route 68, nr Georgetown, OH, USA; GLAHM 101491.

4. *Discina striata* (Schumacher), Recent, Solifor Point, The Gambia.

5. *Discina* sp., Upper Jurassic:
(*a*) Oxfordian/Kimmeridgian, South Ferriby, Humberside, England; **NHM BE274a–b**, **BE307a**.
(*b*) Oxfordian, Ringstead Waxy Clay, Weymouth, Dorset, England; **NHM BE246a–b**, BE263.

6. *Discinisca lamellosa* (Broderip), Recent, Chile.

7. *Discinisca tenuis* (Sowerby), Recent, Swakopmund, Namibia.

8. *Discinisca davisi* Muir-Wood, Tertiary (Middle Eocene, Bracklesham Beds (*Turritella* Bed)), Bracklesham Bay, Sussex, England; NHM BB20391–BB20392.

9. *Discinisca ferroviae* Muir-Wood, Tertiary (Lower Eocene, London Clay (6 feet below the basement beds)), Clapham Brick and Tile Works, Clapham, Sussex, England; NHM B49607.

10. *Discinisca insularis* Muir-Wood, Tertiary (Lower Eocene, London Clay), Alum Bay, Isle of Wight, England; NHM B49612.

11. *Discinisca spitsbergensis* Biernat, Jurassic (Toarcian/Aalenian), Central Spitsbergen; GLAHM 101463.

12. *Discinisca reflexa* (G. B. Sowerby), Lower Jurassic (Upper Toarcian, Blea Wyke Sandstone Formation), Ravenscar, Yorkshire, England; NHM.

13. *Discinisca laevis* (J. de C. Sowerby), Lower Jurassic (Lower Toarcian, Alum Shale Member), Whitby and Ravenscar, Yorkshire, England. NHM B94459, **GLAHM 101450/1**, 101450/2–3, 101451.

14. *Discinisca holdeni* (Tate), Lower Jurassic (Middle Lias), Cheltenham, Gloucestershire, England; **NHM 67715**.
15. *Lindstromella?* sp., Carboniferous (U. Pennsylvanian, Graham Formation), Wayland, TX; GLAHM 101461.
16. *Oehlertella* sp., Early Permian (Tres Saltos Formation), Cerro Colorado del Cementerio, Barreal (Calingasta department), San Juan province, Argentina; GLAHM 101441–101448.
17. *Orbiculoidea koninckii* (Geinitz), Permian (Marl Slate), Thrislington Quarry, Co. Durham, England; GLAHM 101437–101438, **101439–101440**.
18. *Orbiculoidea nitida* (Phillips), Lower Carboniferous:
(*a*) Reedesdale Ironstone Shale, Ridsdale, Northumberland, England; GLAHM L.10454/1–33.
(*b*) Hosie Limestone, High Blantyre, Scotland; GLAHM L320, L5274.
(*c*) Shrimp Bed, Ardross, Scotland; GLAHM.
(*d*) Middle Tournasian, Vegamian Formation, Spain, Cantabrian Mountains; GLAHM 101467–101469.
19. *Orbiculoidea mediorhenana* Fuchs, M. Devonian (Hunsruck Slates), Bundenback, Germany; GLAHM 101464–101466.
20. *Orbiculoidea forbesi* (Davidson), Middle Silurian (Wenlock Shale), Buildwas, Wales; **NHM B1597, B34891**.
21. *Orbiculoidea rugata* (J. de C. Sowerby), Silurian:
(*a*) Wenlock Beds, Rumney (Tymawr Quarry), Wales; **NMW 00.132, G.285**.
(*b*) Wenlock Limestone, Dudley, England; **NMW 00.34**.
(*c*) Elton Beds, Mortimer Forest, Shropshire, England; GLAHM 101449.
22. *Orbiculoidea* sp., Silurian (late Ludlow, Hamra Beds), Vamlingbo, in the vicinity of Vamlingbo Church, Gotland.
23. *Orbiculoidea* sp., Silurian (late Wenlock, Halla Beds), Hörsne, south of Hörsne Church, Gotland.
24. *Orbiculoidea* (?)*gibba* (Lindström), Late Ordovician (Ashgill, Boda Limestone), Dalarna, Sweden.
25. *Pelagodiscus atlanticus* (King), Recent:
(*a*) N. Atlantic, between Iceland and Greenland (64°24′ N, 28°50′ W), 1484 m.
(*b*) N. Atlantic, locality unknown.
(*c*) Atlantic, locality unknown.
(*d*) N. Pacific, locality unknown, 3690 m.
(*e*) Indian Ocean, south of Madagascar (30°23′4″ S, 48°28′5″ E), 4500 m.
26. *Roemerella* sp., Carboniferous (U. Pennsylvanian, Graham Formation), Marietta, TX; GLAHM 101462.
27. *Schizotreta corrugata* Cooper, Ordovician (Pratt Ferry Formation), Pratt Ferry, AL; **GLAHM 101452–101460**, **101492–101493**.

APPENDIX B. METHODS

The protocols for preparing living and fossilized discinoid shells for ultrastructural studies under the SEM including energy dispersive spectrometry (EDX) analysis are those previously adopted (Williams *et al.* 1994, pp. 262–266; Cusack & Williams 1996, p. 36). For amino-acid analysis, manual vapour-phase hydrolysis using 6N HCl was used as described in Cusack & Williams (1996, p. 36). PITC-derivatization of amino acids cannot distinguish between aspartic acid (D) and asparagine (N) or glutamic acid (E) and glutamine (Q). In this context, D–N and E–Q are referred to as acidic amino acids.

(a) *Water and organic content of shells*

For determination of water content, clean valves were powdered in liquid nitrogen and then incubated for 24 h in a desiccator at 30% relative humidity (RH) using a saturated solution of sodium chloride. Valve powders were then heated at 105 °C for 24 h to determine weight loss. Dried shells were further heated at 1100 °C for 1 h to determine organic content.

(b) *Mineral identification*

In view of the great geological range of the materials studied, XRD facilities have been used to monitor any effects of diagenetic recrystallization on fossilized shells. Determinations were made using a Philips PW 1050/35 XRD with a Co energy source ($k\alpha$ 1.7902 Å), Fe filter, vertical coniometer scanning 4°2θ to 60°2θ with a step of 0.02°. Shells were powdered with acetone and poured over glass slides. For samples of low abundance, the shell powders were taken up with liquid paraffin into a fine bore capillary which was then inserted into a Debye–Scherrer camera and the film exposed to X-rays for 3–5 h.

(c) *Microbial contamination*

Additional precautions were taken in preparing fossilized as well as living specimens for chemico-structural studies as normal procedures can lead to microbial contamination. Fossils preserved in fine clastic sediment and analysed in the dried state do not require special procedures (Cusack & Williams 1996). For the present study however, specimens were etched out of carbonate rocks in 5–10% acetic acid. When the specimens were washed free of spent acid and allowed to dry under ambient laboratory conditions they could have become contaminated by bacteria and slime moulds. Accordingly, samples dissolved out of matrix in our laboratories were dried in a laminar flow cupboard immediately after washing and draining.

Micro-organisms have also been identified on shell surfaces of living species that have been prepared for electron microscopy. Their presence prompted consideration of their origin and ways of distinguishing them from GAGs. In section and surface views under the SEM, GAGs are amorphous and moulded to the more rigid parts of the shell but are characterized by artefacts resulting from preparation. Thus, dehydration during the coating of specimens in a vacuum gives rise to contraction depressions within GAGs which can vary from elliptical and subcircular concavities, to grooves up to a micron or more in diameter. Tension cracking of GAGs is also prevalent: but, although triple junctions can occur, one leg is commonly poorly developed or absent and most cracks, about 150 nm or so long, are arcuate possibly as a result of plastic creep of the GAGs after cracking had started. However, GAGs can also occur as discrete discoidal bodies emerging from an apatitic substrate. These bodies fall within the ranges in size and shape of bacteria which have been identified on shell exteriors and internal and fracture surfaces especially within patches of GAGs. Visual identification of many discoidal bodies as

PHILOSOPHICAL TRANSACTIONS OF THE ROYAL SOCIETY B BIOLOGICAL SCIENCES

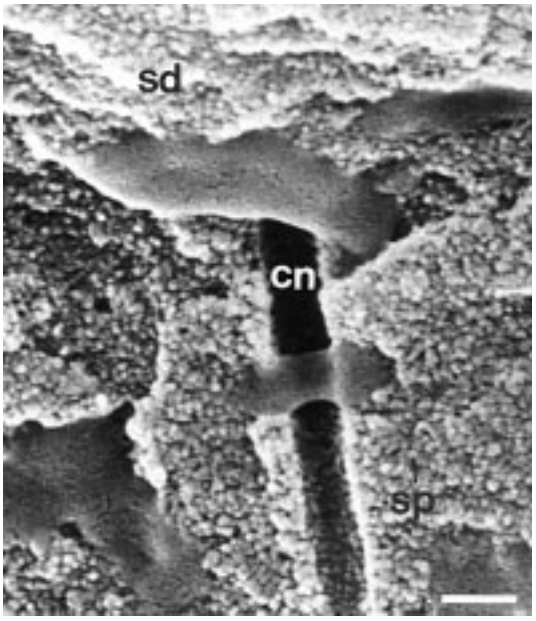

Figure 29. Vertical fracture surface of the secondary layer of the dorsal valve of *Discinisca tenuis*, treated with subtilisin and mounted for SEM study under normal laboratory conditions (see text), showing spherular apatite (sp) of a compact lamina, a stratified lamina (sd) and slime moulds bridging a canal (cn); scale bar, 0.5 µm.

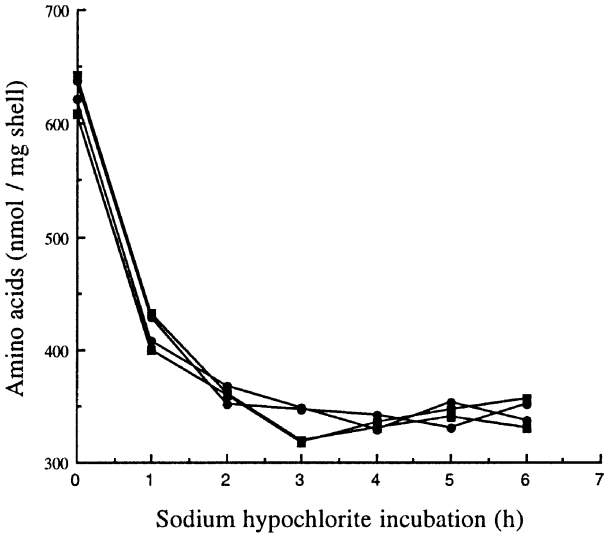

Figure 30. Influence of duration of bleach incubation on level of amino acids extracted by HCl dissolution of *D. tenuis* shells: shell powders were incubated with an aqueous solution of sodium hypochlorite (5% by volume); aliquots were washed free of bleach and dissolved in HCl (2N) and the level of amino acids in each extract was then determined. Two dorsal valves (represented by a circle and a square) were analysed in duplicate.

GAGs, therefore, has had to be checked against a number of criteria.

A survey was made of the distribution of bacteria and GAGs on the external, internal and fracture surfaces of 16 subequal portions of a pair of valves of *D. tenuis*, which had been stripped of tissue *in vivo* and preserved in 70% ethanol. The portions were treated with enzymes in a clean room. A total of six and five portions were incubated with subtilisin and proteinase-K, respectively, and the remaining five controls were kept in a phosphate buffer. Within 24 h all had been mounted on stubs under normal laboratory conditions and then shadowed with gold.

Some bacteria were found, especially on external surfaces, and were distinguishable by the shape and rigidity of their capsules which were not indented by contiguous apatitic spherules in the substrate, although they were commonly flattened medially and even perforated, presumably by implosion of empty capsules during their shadowing under a vacuum. A total of four morphological types were seen: straight (exceptionally with fibrils) and comma-shaped rods, cocci, and motile cylindroids with single polar flagella; all were identified on surfaces treated with subtilisin and proteinase-K. Elongately ellipsoidal to parallel-sided bodies with shallow medial depressions also occurred, commonly less than 1.5 µm long, which looked like GAGs but acted like bacteria (figure 29). These bodies were not contained in rigid capsules so that they were indented peripherally by apatitic spherules and were moulded to breaks of slope. They also bridged canals in laboratory-prepared fracture surfaces. The presence of these flaccid structures on buffered section surfaces precludes their having been blebs of GAGs dislodged during enzymic digestion. They have been temporarily identified as slime moulds that disconcertingly look like flattened vesicular discharges of GAGs under the SEM. Such blebs of GAGs, however, have been distinguished in this study by the lack of definite boundaries between contiguous constituents, the occurrence of partly engulfed spherules well within their peripheries and their occasional penetration by canals (see figure 2*a*).

Although microbial infestations on section surfaces were very rare and localized within areas less than 100 µm^2, they included motile cylindroids resembling marine thiopneute bacteria and they, at least, could have entered damaged shells *in vivo*. Accordingly, to distinguish between bacteria which were present in the shell of *D. tenuis* at the time of collection and those that contaminated specimens during preparation, portions of two dorsal valves, incubated in the clean room, were dried and mounted on SEM stubs in a laminar flow cabinet and gold-coated immediately after.

Micro-organisms were not found on the surfaces of sections only on valve exteriors, especially in hollows bound by superficial lamellae and in the vicinity of the pedicle opening in the ventral valve, where bacteria were associated with diatoms and oocytes.

In view of the microbial occupancy of the exteriors of living *D. tenuis*, these lamellose surfaces were thoroughly scrubbed before shells were powdered and incubated with an aqueous solution of sodium hypochlorite (5% by volume). Figure 30 shows that, after 3 h of incubation with bleach, much of the organic material is destroyed, the remainder being protected by interaction with the mineral. In subsequent analyses, shell powders of *D. tenuis* were incubated in this way for 4 h compared with 1 h for other species.

(d) *Extraction of mineral-associated proteins of* D. tenuis

Following removal of the sodium hypochlorite, extraction of mineral-associated EDTA-soluble proteins was

carried out as described in Williams *et al*. (1994) although, with *D. tenuis*, exhaustive dissolution by incubation with EDTA (20%, pH 8) in a ratio of 23 ml EDTA solution per gramme of shell lasted for 20 days to maximize protein extraction.

Protein extracts were examined by SDS-PAGE (15% polyacrylamide) using the method of Schägger & Von Jagow (1987). Proteins were either visualized in polyacrylamide gels by staining with Coomassie Brilliant Blue or electroblotted onto ProBlott membrane and visualized by Coomassie staining before amino-acid analysis of the purified proteins. Duplicate electroblots were also prepared in which sugar groups were detected by lectin binding using concanavalin A-peroxidase in the method of Faye & Chrispeels (1985).

(e) *Tablets of larval valves of* D. tenuis

Larval shells of *D. tenuis* were washed in 18 MΩ water for 1 h and then incubated in an aqueous solution of sodium hypochlorite (1% by volume) for 60 h. A total of four larval valves were then examined by SEM to determine the extent to which tablets had been removed from the valve surface. The hypochlorite solution, the water wash and a further solution of hypochlorite which had not been in contact with the shells, were all concentrated by centrifugation under vacuum. A small precipitate formed in the bleach solution which had been in contact with the shells. The three solutions and the resuspended precipitate were then dried onto XRD slides and analysed as described.

D. tenuis shells were fixed on glass slides using Buehler epoxy resin and then carbon coated. Electron microprobe analyses were obtained using a Camebax SX-50 with four spectrometers operated with a 15 kV accelerating voltage, a 20 nA beam current and a 5 μm spot size.

APPENDIX C. DATA USED IN PHYLOGENETIC ANALYSIS

(a) *The states of 38 characters used in the phylogenetic analysis of nine discinoid and three other lingulide genera listed in Appendix C(b)*

shell shape	
1. growth:	holoperipheral (0), mixoperipheral (1), hemiperipheral (2)
2. convexity:	biconvex (0), dorsibiconvex (1), planoconvex (2), ventribiconvex (3), convexoconcave (4)
3. larval pedicle opening:	absent (0), marginal notch (1), within valve (2)
4. adult pedicle notch:	absent (0), obtusely divergent (1), narrow to parallel (2)
5. posterior pedicle notch:	absent (0), open (1), closed by periostracum (2), closed by shell (3)
6. listrium:	absent (0), poorly developed (1), present (2)
7. external pedicle tube:	absent (0), present (1)
8. internal pedicle tube:	absent (0), present (1)
9. ventral pseudointerarea:	absent (0), present (1), 'acrotretoid' (2)
10. dorsal pseudointerarea:	absent (0), present (1)
11. dorsal umbo:	marginal (0), posterior (1), subcentral (2)
12. ventral umbo:	marginal (0), posterior (1), subcentral (2)
ornamentation	
13. larval shell:	smooth (0), pitted (1), tablets (2)
14. tablet distribution:	absent (0), open-packed (1), close-packed (2)
15. adult shell:	smooth (0), vesicular (1)
16. superficial pits:	absent (0), present (1)
17. costellae:	absent (0), present (1)
18. capillae:	absent (0), present (1)
19. fila:	absent (0), present (1)
20. external lamellae:	absent (0), present (1)
musculature	
21. ventral posterior adductor scars:	paired, posteriomedian (0), paired, posteriolateral (1), paired subcentral (2), absent (3), unpaired, posteriolateral (4)
22. ventral transmedian scars:	symmetrical (0), asymmetrical (1)
23. ventral posteriolateral muscle fields:	anterior to umbo (0), posterior to umbo (1), on inner sides of acrotretoid pseudointer area (2)
24. dorsal outside lateral muscle scars:	absent (0), present (1), combined with middle lateral scars (2)
25. dorsal anterior adductor scars:	absent (0), present (1)
26. ventral medial septum:	absent (0), present (1), apical process (2)
27. dorsal ridge:	absent (0), present (1), as septum (2), with buttress (4)
mantle canal systems	
28. ventral:	baculate (0), bifurcate (1), pinnate (2)
29. dorsal:	baculate (0), bifurcate (1), pinnate (2)
30. dorsal *vascula media*:	absent (0), present (1)

(*Cont.*)

Appendix C(a). (*Cont.*)

shell structure	
31. baculae:	absent (0), present in both valves (1), ventral valve only (2), incipient (3)
32. baculate sets:	absent–incipient (0), with compact floor and ceiling (1), cyclical (2), variable (3)
33. canal system:	absent (0), present (1), present in ventral valve (2)
34. tubercles:	absent (0), present (1)
35. columnar/camerate sets:	absent (0), present (1)
36. periostracal superstructure:	absent/other (0), sheeted (1), sheeted with ridges (2)
37. matrix of baculate sets:	absent (0), mainly GAGs (1), GAGs with apatite (3)
38. vesicular pits:	absent (0), large, simple (1), large composite (2), small, simple (3), small, simple, sporadic (4)

(b) *Matrix of 38 characters listed in Appendix C (a)*, among nine discinoid and three other lingulide genera

	[11		11111111222222222333333333
	12345678901		23456789012345678901234567 8]
Rowellella	11000000110		00010000100011000010 0?00003
Acrotetra	03200001210		21000001000221232200 0?01010
Discina	00123001002		22100110000111101111210 0210
Discinisca	00122200002		22100010100111101112211 0210
Pelagodiscus	00123?00002		22210011000111001113020 0104
Schizotreta	00123201000		10010001000111001111?00011
Orbiculoidea	0112320100	(12)	20010001000111001111210 0022
Lindstroemella	01121?0?002		20010001000111011111 2?00022
Roemerella	04123?0?002		20010001000111001111 2?00022
Trematis	01111100010		20001000?????101???10?00000
Schizocrania	10000000110		20000100?????100???30?00000
Pseudolingula	10000000110		00000000000021010001 3?000?0

REFERENCES

Biernat, G. & Williams, A. 1970 Ultra-structure of the protegulum of some acrotretide brachiopods. *Palaeontology* **13**, 491–502.

Chuang, S. H. 1977 Larval development of *Discinisca* (inarticulate brachiopod). *Am. Zool.* **17**, 39–53.

Cusack, M. & Williams, A. 1996 Chemico-structural degradation of Carboniferous lingulid shells. *Phil. Trans. R. Soc. Lond.* B **351**, 33–49.

Faye, L. & Chrispeels, M. J. 1985 Characterization of *N*-linked oligosaccharides by affinoblotting and treatment of the blots with glycosidases. *Ann. Biochem.* **149**, 218–224.

Holmer, L. E. 1986 Inarticulate brachiopods around the Middle–Upper Ordovician boundary in Västergötland. *Geol. Fören. Forhandl.* **108**, 97–126.

Holmer, L. E. 1987 Discinacean brachiopods from the Ordovician Kullsberg and Boda limestones of Dalarna, Sweden. *Geol. Fören. Forhandl.* **109**, 317–326.

Holmer, L. E. 1989 Middle Ordovician phosphatic inarticulate brachiopods from Västergötland and Dalarna, Sweden. *Fossils Strata* **26**, 1–172.

Holmer, L. E. & Popov, L. E. 1994 Revision of the type species of *Acrotreta* and related lingulate brachiopods. *J. Paleont.* **68**, 433–450.

Holmer, L. E. & Popov, L. E. 1996 Early Palaeozoic radiation and classification of organo-phosphatic brachiopods. In *Brachiopods. Proc. Third Int. Brachiopod Congr., Sudbury (Ontario), Canada, 2–5 September 1995* (ed. P. Copper & J. Jin), pp. 117–121. Rotterdam: A. A. Balkema.

Iijima, M., Hiroko, T., Yutaka, M. & Yoshinori, K. 1991 Difference of the organic component between the mineralized and the non-mineralized layers of *Lingula* shell. *Comp. Biochem. Physiol.* A **98**, 379–382.

Iwata, K. 1981 Ultrastructure and mineralization of the shell of *Lingula unguis* Linne (inarticulate brachiopod). *J. Faculty Sci. Hokkaido Univ.* IV **20**, 35–65.

Iwata, K. 1982 Ultrastructure and calcification of the shells in inarticulate brachiopods. 2. Ultrastructure of the shells of *Glottidia* and *Discinisca*. *J. Geol. Soc. Jap.* **88**, 957–966.

Jope, H. M. 1965 Composition of brachiopod shell. In *Treatise on invertebrate paleontology*, part H (ed. R.C. Moore), pp. H156–164. Kansas: Geological Society of America and University of Kansas Press.

Jope, H. M. 1980 Phylogenetic information derivable from fossil brachiopods. In *Biogeochemistry of amino acids* (ed. P. E. Hare, T. C. Hoering & K. King Jr), pp. 83–94. New York: Wiley.

Le Geros, R. Z., Pan, C.-M., Suga, S. & Watabe, N. 1985 Crystallo-chemical properties of apatite in atremate brachiopod shells. *Calc. Tissue Int.* **37**, 98–100.

Lowenstam, H. A. & Weiner, S. 1989 *On biomineralization*. New York: Oxford University Press.

Morrisey, J. H. 1981 Silver stain for proteins in polyacrylamide gels: a modified procedure with enhanced uniform sensitivity. *Ann. Biochem.* **117**, 307–310.

Pan, C.-M. & Watabe, N. 1988 Shell growth of *Glottidia pyramidata* Stimpson (Brachiopoda: Inarticulata). *J. Exp. Mar. Biol. Ecol.* **119**, 257–268.

Popov, L. E. 1992 The Cambrian radiation of brachiopods. In *Origin and early evolution of metazoa* (ed. J. H. Lipps & P. W. Signor), pp. 399–423. New York: Plenum.

Popov, L. E. & Ushatinskaya, G. T. 1992 Lingulidy, proiskhozhdenie discinids, sistematika bysokikh taksonoov. In *Drevneishie brakhiopody territorii severnoi Evrazil* (ed. L. N. Repina & A. Yu. Rozanov), pp. 59–67. Novosibirsk: Akademiya Nauk.

Poulsen, V. 1971 Notes on an Ordovician acrotretacean brachiopod from the Oslo region. *Bull. Geol. Soc. Denm.* **20**, 265–278.

Schägger, H. & Von Jagow, G. 1987 Tricine-sodium dodecyl sulfate-polyacrylamide gel electrophoresis for the separation of proteins in the range from 1 to 100 kDa. *Ann. Biochem.* **166**, 368–379.

Swofford, D. L. & Begle, D. P. *1993 PAUP, phylogenetic analysis using parsimony, version 3.1.* User's Manual. Laboratory of Molecular Systematics, Smithsonian Institution.

Westbroek, P., de Jong, E. W., van der Wal, P., Borman, A. H., de Vrind, J. P. M., Kok, D., de Bruijn, W. C. & Parker, S. B. 1984 Mechanism of calcification in the marine alga *Emiliania huxleyi*. *Phil. Trans. R. Soc. Lond.* B **304**, 435–444.

Williams, A. 1971 Comments on the growth of the shell of articulate brachiopods. *Smiths. Contrib. Paleobiol.* **3**, 47–67.

Williams, A. & Curry, G. B. 1991 The microarchitecture of some acrotretide brachiopods. In *Brachiopods through time* (ed. D. I. MacKinnon, D. E. Lee & J. D. Campbell), pp. 133–140. Rotterdam: A. A. Balkema.

Williams, A. & Holmer, L. E. 1992 Ornamentation and shell structure of acrotretoid brachiopods. *Palaeontology* **35**, 657–692.

Williams, A. & Mackay, S. 1979 Differentiation of the brachiopod periostracum. *Palaeontology* **22**, 721–736.

Williams, A. & Rowell, A. J. 1965 Classification. In *Treatise on invertebrate paleontology*, part H (ed. R. C. Moore), pp. H214–234. Kansas: Geological Society of America and University of Kansas Press.

Williams, A., Mackay, S. & Cusack, M. 1992 Structure of the organo-phosphatic shell of the brachiopod *Discina*. *Phil. Trans. R. Soc. Lond.* B **337**, 83–104.

Williams, A., Cusack, M. & Mackay, S. 1994 Collagenous chitinophosphatic shell of the brachiopod *Lingula*. *Phil. Trans. R. Soc. Lond.* B **346**, 223–266.

Williams, A., Cusack, M., Buckman, J. O. & Stachel, T. 1998*a* Siliceous tablets in the larval shells of apatitic discinid brachiopods. *Science* **279**, 2094–2096.

Williams, A., Popov, L. E., Holmer, L. E. & Cusack, M. 1998*b* The diversity and phylogeny of the paterinate brachiopods. *Palaeontology* **41**, 221–262.

Wright, A. D. 1981 The external surface of *Dictyonella* and of other pitted brachiopods. *Palaeontology* **24**, 443–481.

PHILOSOPHICAL TRANSACTIONS OF THE ROYAL SOCIETY B BIOLOGICAL SCIENCES